MARTIN MARIETTA ENERGY SYSTEMS LIBRARIES
3 4456 0360670 1

CENTRAL RESEARCH LIBRARY
DOCUMENT COLLECTION

ORNL 1598
4a
Engineering

THE EFFECT OF VISCOSITY UPON THE PRESSURE DISTRIBUTION FOR SWIRLING FLOW THROUGH A RIGHT CIRCULAR CYLINDER

R. H. Wilson

OAK RIDGE NATIONAL LABORATORY
CENTRAL RESEARCH LIBRARY
DOCUMENT COLLECTION

LIBRARY LOAN COPY

DO NOT TRANSFER TO ANOTHER PERSON

If you wish someone else to see this document, send in name with document and the library will arrange a loan.

OAK RIDGE NATIONAL LABORATORY
OPERATED BY
CARBIDE AND CARBON CHEMICALS COMPANY
A DIVISION OF UNION CARBIDE AND CARBON CORPORATION
UCC
POST OFFICE BOX P
OAK RIDGE, TENNESSEE

ORNL 1598

This document consists of 83 pages.
Copy 12 of 305 copies. Series A.

Contract No. W-7405-eng-26

REACTOR EXPERIMENTAL ENGINEERING DIVISION

THE EFFECT OF VISCOSITY UPON THE PRESSURE DISTRIBUTION FOR SWIRLING FLOW THROUGH A RIGHT CIRCULAR CYLINDER

R. H. Wilson

DATE ISSUED
AUG 24 1953

OAK RIDGE NATIONAL LABORATORY
Operated by
CARBIDE AND CARBON CHEMICALS COMPANY
A Division of Union Carbide and Carbon Corporation
Post Office Box P
Oak Ridge, Tennessee

ORNL 1598
Engineering

INTERNAL DISTRIBUTION

1. C. E. Center
2. Biology Library
3. Health Physics Library
4-5. Central Research Library
6. Reactor Experimental Engineering Library
7-11. Laboratory Records Dept.
12. Laboratory Records, ~~ORNL-R.C.~~
13. C. E. Larson
14. W. B. Humes (K-25)
15. L. B. Emlet (Y-12)
16. A. M. Weinberg
17. E. H. Taylor
18. E. D. Shipley
19. C. E. Winters
20. F. C. VonderLage
21. R. C. Briant
22. J. A. Swartout
23. S. C. Lind
24. F. L. Culler
25. A. H. Snell
26. A. Hollaender
27. M. T. Kelley
28. W. J. Fretague
29. G. H. Clewett
30. K. Z. Morgan
31. T. A. Lincoln
32. A. S. Householder
33. C. S. Harrill
34. D. S. Billington
35. D. W. Cardwell
36. E. M. King
37. R. N. Lyon
38. A. J. Miller
39. R. B. Briggs
40. A. S. Kitzes
41. O. Sisman
42. R. W. Stoughton
43. C. B. Graham
44. W. R. Gall
45. H. F. Poppendiek
46. S. E. Beall
47. J. P. Gill
48. D. D. Cowen
49. R. A. Charpie
50. R. E. Aven
51. E. G. Bohlmann
52. R. H. Chapman
53. J. A. Hafford
54. J. A. Lane
55. L. B. Lesem
56. I. Spiewak
57. R. H. Wilson
58. M. Beckner
59. F. N. Peebles (consultant)
60. W. M. Breazeale (consultant)
61. M. J. Skinner

EXTERNAL DISTRIBUTION

62. D. B. Benedict, C&CCC, South Charleston
63. R. F. Bacher, California Institute of Technology
64-305. Given distribution as shown in TID-4500 under Engineering category

DISTRIBUTION PAGE TO BE REMOVED IF REPORT IS GIVEN PUBLIC DISTRIBUTION

TABLE OF CONTENTS

CHAPTER		PAGE
I.	SUMMARY	1
II.	INTRODUCTION	3
III.	LITERATURE SURVEY	5
IV.	EQUIPMENT	14
V.	EXPERIMENTAL PROCEDURE	20
VI.	RESULTS AND CONCLUSIONS	23
LIST OF REFERENCES		52
BIBLIOGRAPHY		53
APPENDIX		58
NOMENCLATURE		77

LIST OF TABLES

TABLE		PAGE
I.	Summary of Pressure Distribution Data for Water with 0.308 Inch Inlets	30
II.	Summary of Pressure Distribution Data for SAE 10 Oil with 0.308 Inch Inlets	32
III.	Summary of Pressure Distribution Data for SAE 10 Oil with 0.147 Inch Inlets	33
IV.	Summary of Pressure Distribution Data for SAE 60 Oil with 0.147 Inch Inlets	34
V.	Summary of Pressure Distribution Data for Water with 0.147 Inch Inlets	35
VI.	The Variation of α with Viscosity	38
VII.	Residence Times for Water in the Cylinder	43
VIII.	Pressure Distributions for Various Probe Insertions	47
IX.	Orifice Calibration	63
X.	Orifice Data and Physical Properties for Oils	64
XI.	Pressure Distribution Data for All Runs	65
XII.	Residence Times for Water in the Cylinder	76

LIST OF FIGURES

FIGURE		PAGE
1.	Cylindrical Test Section	15
2.	Top of Cylindrical Test Section	16
3.	Photograph of Apparatus	17
4.	Flow Diagram for Apparatus	18
5.	Pressure Profiles for Water Using 0.308 Inch Inlets	25
6.	Pressure Profiles for SAE 10 Oil Using 0.308 Inch Inlets	26
7.	Pressure Profiles for SAE 10 Oil Using 0.147 Inch Inlets	27
8.	Pressure Profiles for SAE 60 Oil Using 0.147 Inch Inlets	28
9.	Pressure Profiles for Water Using 0.147 Inch Inlets	29
10.	Effect of Viscosity on the Ratio of Peripheral Velocity to Inlet Velocity	37
11.	Residence Times for Water in Cylinder	42
12.	Effect of Probe on Pressure Distribution	45
13.	Effect of Probe on Velocity Profile	46

CHAPTER I

SUMMARY

A laboratory study and literature survey were carried out concurrently in an effort to determine the effect of viscosity upon the pressure and velocity distributions in a vortex formed by swirling flow through a cylindrical vessel. References are cited which show the conflicting views of various authors with regard to the effect of fluid friction upon the nature of the flow of real fluids in a vortex. In the laboratory water and two hydrocarbon oils, SAE 10 and SAE 60, were studied under conditions of swirling flow in a right circular cylinder. Pressure distributions for all three liquids were found to fit the equation

$$\Delta P = \frac{\rho V_R^2}{2 g_c} \left[\left(\frac{R}{r} \right)^2 - 1 \right]$$

where

ΔP = pressure drop from R to r, lb. force/ft.^{2}

ρ = density, lb. mass/ft.^{3}

V_R = effective peripheral velocity, ft./sec.

g_c = conversion factor, lb. mass x ft./sec.^{2} lb. force

R = cylinder radius, ft.

r = position radius, ft.

Such a correlation shows that angular momentum is conserved within the vortices studied and that the velocity distribution is given by the equation

$$v\ r = C, \text{ a constant.}$$

The fluid friction did not cause the pressure distribution to depart perceptibly from that of a free vortex. However the effect of fluid friction was detectable by contrasting the effective peripheral velocity with the inlet velocity. The greater the viscosity, the smaller was the ratio,

$$\alpha = \frac{V_R}{V_i}$$

where V_i = inlet velocity, ft./sec.

Injection of dye into the cylinder revealed that the residence time of some liquid in the cylinder was 3.86 times the calculated residence time, based on slug flow through the cylinder volume. This confirmed the existence of secondary flow patterns within the vessel.

Observation of the pressure distribution during the use of a velocity probe indicated that the velocity distribution was altered appreciably by the presence of the probe.

CHAPTER II

INTRODUCTION

Swirling flow as a centrifugal separation process is a familiar subject in engineering practice. Perhaps the most widely known use for swirling flow is in the separation of dusts or mists from gas streams within such equipment as the cyclone separator. In recent years the same type of separator has been found useful for the separation and classification of solid particles suspended in liquids. The coal industry in particular has utilized the liquid-solid cyclone in coal washing and in the recovery of coal fines that would otherwise be waste.

Much empirical data and qualitative information have been published about centrifugal separators using swirling flow, while relatively little fundamental knowledge about the nature of the flow within the swirl, or vortex, is available. A survey of the most outstanding publications pertaining to fundamental study of swirling flow is found in Chapter III. In the articles cited it is apparent that there is conflicting information with regard to the effect of the fluid viscosity upon the flow pattern in a liquid undergoing the process called swirling flow. The term swirling flow as used here connotes the movement of fluid radially through a vortical region from a source in the periphery of a vortex to a sink at the axis of the vortex. The peripheral source is usually a tangential inlet.

The conflicting information in the literature cited has given rise to this investigation. It was desired to know the effect of viscosity and liquid shear upon the pressure and velocity distributions in a vortex associated with swirling flow. Such knowledge will assist in the design of hydraulic equipment utilizing swirling flow.

In this study three liquids were employed to show the influence of viscous forces on the swirling flow in a right circular cylinder. These were water and two hydrocarbon oils, designated as SAE 10 and SAE 60. Radial pressure distribution measurements were made with each of these liquids for various flow conditions. Such data were analyzed to determine the effect of viscosity on the swirling flow within the cylindrical vessel.

Chapters IV, V and VI describe the equipment used in this study, the experimental procedures used and the various experimental results. Chapter VI also contains a discussion of the results and conclusions derived from the study.

CHAPTER III

LITERATURE SURVEY

One of the most sought after correlations for vortical flow has been an accurate expression for the tangential velocity as a function of radius. Empirical work has been done on this subject by several investigators. The measurements in question were made in cyclone separators, and the data fit the equation,

$$v\, r^n = C \tag{1}$$

where

v = tangential velocity

r = radial distance from the axis of rotation

n, C = constant

There is some degree of agreement among the various investigators on the values for n. The values fall in the interval 0.5 to 0.9 for a wide range of conditions. Shepherd and Lapple (16, 17)* and also Stairmand (18) found that n = 0.5 fit their data obtained by pitot tube measurements for gas flow in a cyclone. Alexander (1) also quotes values for n. They range from 0.5 to 0.75. Saito and Ito (15) in Japan studied the paths of balls (specific gravity = 1.0) in a water vortex and found that n = 0.61. However they

---

*Numbers following authors' names indicate items in the List of References.

had reason to doubt that the balls travelled at the same velocity as the water. Kelsall (11) found from his water-flow data in a cyclone that n had values ranging from 0.75 to 0.84. He used aluminum particles in the water, and optical methods were used to determine the velocity. Other authors (3, 12) of works on cyclone separators have assumed or found from their experience that n = 1, which gives the potential flow equation for two-dimensional vortical flow,

$$v\ r = C \tag{2}$$

In these cases, however, it should be stated that the effective peripheral velocity in the cyclone is different from the inlet velocity.

There have been diverse opinions about the theory of shear in circular flow. Wattendorf (21) reviewed the momentum transport theory of Prandtl, and concluded that for circular flow

$$\tau \propto \frac{d\,v}{d\,r} + \frac{v}{r} \tag{3}$$

τ = local specific shear stress

Taylor (20) developed the vorticity transport theory which gives as a result that

$$\tau \propto \frac{d\,v}{d\,r} - \frac{v}{r} \tag{4}$$

It is noticed that equation (4) is at variance with equation (3). In order to determine the relative validity of the two conclusions, similar experiments were performed and cited by both Wattendorf and Taylor (19). The experimental apparatus consisted of two concentric

cylinders mounted in such manner that water was contained in the annulus while the inner cylinder was rotated at known speeds. Pressure and velocity measurements were made. The data revealed that

$$v\ r = C \tag{2}$$

for the interior regions of the fluid over the greater part of the annular thickness. However, near the walls, there was considerable departure from equation (2); viz., an increase of v r near the inner wall and a decrease of v r near the outer wall. Both Wattendorf and Taylor seemed to agree that the momentum transport theory held near the walls, and the vorticity transport theory held in the interior. Kassner (10) objected to this compromise and maintained that Prandtl made an error in his development, this error being that Prandtl considered only particles that had the average value for the moment of momentum of all the particles in the cylindrical element under consideration. The result of Kassner's correction is that both theories yield

$$\tau \propto \frac{d\ v}{d\ r} - \frac{v}{r} \tag{4}$$

It is not claimed that the theories are identical, but rather that they supplement each other. The shear is proportional to the sum of the vorticity transfer and the momentum transfer, and each is proportional to $\frac{d\ v}{d\ r} - \frac{v}{r}$. An interesting point about the shear in irrotational flow is presented by Kassner. Since for laminar flow,

$$\tau = \mu \left[\frac{d\,v}{d\,r} - \frac{v}{r} \right] \tag{5}$$

where μ = molecular viscosity

Assuming an irrotational flow where

$$v\,r = C \text{ or } v = \frac{C}{r} \tag{2}$$

the result is that

$$\tau = \mu \left[- \frac{C}{r^2} - \frac{C}{r^2} \right] = - 2\mu \frac{C}{r^2} = - 2\,\mu \frac{v}{r} \tag{6}$$

The shearing moment, M, on the surface of a cylindrical element of unit height is

$$M = \tau \cdot 2\,\pi\,r^2 \tag{7}$$

$$M = - 2\,\mu \frac{C}{r^2} \cdot 2\,\pi\,r^2 = - 4\,\pi\,\mu\,C, \text{ a constant} \tag{8}$$

For turbulent flow μ is replaced by $\mathcal{E}$ to give

$$M = - 4\,\pi\,\mathcal{E}\,C, \text{ a constant} \tag{9}$$

One other interesting point is a discussion by Kassner of the condition for steady circular flow of viscous fluids. Since

$$\tau \cdot 2\,\pi\,r^2 = \text{a constant}, \tag{10}$$

$$\left[\frac{d\,v}{d\,r} - \frac{v}{r} \right] r^2 = \text{a constant} \tag{11}$$

and

$$\frac{d}{dr}\left(\frac{v}{r}\right) = \frac{\text{a constant}}{r^3} \tag{12}$$

The general solution of (12) is

$$v = \frac{C_9}{r} + C_{10}\,r \tag{13}$$

The velocity of irrotational flow, $\frac{C_9}{r}$, is a solution because it represents flow with a constant moment of friction stresses, and the velocity of rotational flow, $C_{10}\, r$, is a solution because it has no friction stresses. A similar development is also given by Green (8). The work of Kassner and Knoernschild (10) is reviewed in a clear and concise manner by Fulton (5).

Einstein and Li (4) have made one of the most complete studies of vortical flow in a cylinder to date for a single fluid, water. The theoretical development of velocity equations begins with the equations of Navier and Stokes and the continuity equation written using cylindrical coordinates.

Navier-Stokes equations:

$$\frac{\partial u}{\partial t} + u\frac{\partial u}{\partial r} + \frac{v}{r}\frac{\partial u}{\partial \phi} + w\frac{\partial u}{\partial z} - \frac{v^2}{r} = -\frac{1}{\rho}\frac{\partial p}{\partial r} + \nu\left[\nabla^2 u - \frac{u}{r^2} - \frac{2}{r^2}\frac{\partial v}{\partial \phi}\right] \qquad (14)$$

$$\frac{\partial v}{\partial t} + u\frac{\partial v}{\partial r} + \frac{v}{r}\frac{\partial v}{\partial \phi} + w\frac{\partial v}{\partial z} + \frac{uv}{r} = -\frac{1}{\rho}\cdot\frac{1}{r}\frac{\partial p}{\partial \phi} + \nu\left[\nabla^2 v + \frac{2}{r^2}\cdot\frac{\partial u}{\partial \phi} - \frac{v}{r^2}\right] \qquad (15)$$

$$\frac{\partial w}{\partial t} + u\frac{\partial w}{\partial r} + \frac{v}{r}\frac{\partial w}{\partial \phi} + w\frac{\partial w}{\partial z} = -\frac{1}{\rho}\frac{\partial p}{\partial z} + \nu\nabla^2 w \qquad (16)$$

$$\nabla^2 = \frac{\partial^2}{\partial r^2} + \frac{1}{r}\frac{\partial}{\partial r} + \frac{1}{r^2}\frac{\partial^2}{\partial \phi^2} + \frac{\partial^2}{\partial z^2}$$

Equation of continuity:

$$\frac{1}{r}\frac{\partial (ru)}{\partial r} + \frac{1}{r}\frac{\partial v}{\partial \phi} + \frac{\partial w}{\partial z} = 0 \qquad (17)$$

where

u = radial velocity

w = vertical velocity

ϕ = angular distance

z = vertical distance

t = time

ρ = density

p = pressure

$\nu = \frac{\mu}{\rho}$ = kinematic viscosity

∇ = Laplacian operator

The following assumptions are made:

1. The system operates under steady-state conditions.
2. Rotation is symmetrical with respect to the Z-axis, which coincides with the axis of the vessel.
3. The radial component of velocity is uniform at any given radius in the outer region ($r_2 \leq r \leq R$).
4. The vertical velocity w is uniform at any given height Z in the core region ($0 \leq r \leq r_2$).

For the outer region equations (17) and (15) combine and reduce to

$$r^2 \frac{d^2v}{dr^2} + (\beta + 1) r \frac{dv}{dr} + (\beta - 1) v = 0 \tag{18}$$

where

$$\beta = \frac{V_o \rho}{2 \pi h \mu} \tag{19}$$

V_o = volumetric flow rate

h = height of cylinder

The solutions are

$$v = C_1 r^{(1-\beta)} + C_2 r^{-1}; \ \beta \neq 2 \tag{20}$$

$$v = \frac{C_3}{r} + \frac{C_4}{r} \ln r \ ; \ \beta = 2 \tag{21}$$

For the core region equations (17) and (15) reduce to

$$v = \frac{1}{r}\left[C_5 + C_6 \, e^{-\frac{\beta r^2}{2 r_2^2}}\right] \tag{22}$$

The following boundary conditions are used:

At $r = R$, $v = V_R$.

At $r = 0$, v is finite.

At $r = r_2$, $\beta \neq 2$; $\frac{d}{dr}\left(\frac{v}{r}\right)$ has the same value for both equations (20) and (22).

The case $\beta = 2$ was considered rare and hence was not carried through to a final expression. For the case $\beta \neq 2$ the constants were evaluated. For the outer region the result is

$$\frac{rv}{RV_R} = \frac{\left[\beta-2 \ (1-e^{-\beta/2})\right] \left[1 - \left(\frac{r}{R}\right)^{-(\beta-2)}\right]}{\beta\left[1-e^{-\beta/2}\left(\frac{r_2}{R}\right)^{\beta-2}\right]-2\left[1-e^{-\beta/2}\right]} + \left(\frac{r}{R}\right)^{-(\beta-2)} \tag{23}$$

For the core region the result is

$$\frac{rv}{RV_R} = \frac{\left[\beta-2\right]\left[1-e^{-\frac{\beta}{2}\left(\frac{r}{r_2}\right)^2}\right]}{\beta\left[1-e^{-\beta/2}\left(\frac{r_2}{R}\right)^{\beta-2}\right]-2\left[1-e^{-\beta/2}\right]} \tag{24}$$

R = cylinder radius

V_R = peripheral velocity

r_2 = outlet radius

Experimental data were obtained from a water vortex in a cylindrical tank, and these data were used to evaluate β. The values of β as determined from the experiment were two and five, and were orders of magnitude smaller than the values of β determined from equation (19) using the molecular viscosity. It was explained that this discrepancy may be due to turbulence and the effects of the eddy viscosity ϵ . It was thought that a more proper expression for β would be given by

$$\beta = \frac{V_o \rho}{2 \pi h (\mu + \epsilon)} \tag{25}$$

Utilizing the same method as that shown by Einstein and Li, Garber and Peebles (6) investigated vortical flow in a sphere. Pressure distribution data for swirling flow in an eight-inch sphere were obtained in the laboratory and used to determine a value for β. The value given is 2.1, which is smaller by a factor of 10^3 than the value given by the expression

$$\beta = \frac{V_o \rho}{4 \pi R' \mu} \tag{26}$$

where

R' = sphere radius.

This discrepancy was attributed to turbulence, which was not accounted for in the equations used. Expressions for laminar flow were used as a first approach to the problem.

Daugherty (2) gives an idea of the relative magnitudes of turbulent viscosity as compared to molecular viscosity. He has

stated that the turbulent viscosity may have a value 20,000 times that of the molecular viscosity for the given fluid.

Russell (14) presented a derivation for a very useful differential equation. His analysis considers the balance of forces on an element of fluid in a vortex and arrives at the equation

$$d\,A\,dp = d\,A\,dr\,\frac{\rho}{g_c}\,\frac{v^2}{r} \tag{27}$$

which reduces to

$$dp = \frac{\rho}{g_c}\,\frac{v^2}{r}\,dr \tag{28}$$

dA = an elemental area

If v as a function of r be known, the pressure distribution can be computed. It is noted that if viscous effects and the radial velocity are small compared to the tangential velocity, equation (14) reduces to equation (28).

CHAPTER IV

EQUIPMENT

The test section was the cylinder whose dimensions are shown in Figure 1. Inside dimensions were approximately eight inches for the diameter and six inches for the depth. The inlets were two narrow rectangular openings 180° apart that extended the full depth of the cylinder. The inlet passages were attached to the cylinder in such a manner that the liquid entered tangentially. At the beginning of the experiments the average inlet width was 0.308 inches, and later it was changed to 0.147 inches in order to obtain higher velocities with the same flow. The pressure taps were drilled in the transparent plastic top of the cylinder as shown in Figure 2. Nine holes 0.032 inches in diameter were spaced so as to give the static pressure distribution from the cylinder wall to within one sixteenth of an inch of the two-inch outlet channel. Two holes 0.032 inches in diameter served as pressure taps in the outlet channel.

The liquid was circulated by a Wilfley centrifugal pump rated at two hundred gallons per minute at one hundred pounds per square inch. A photograph of the whole system is shown in Figure 3, and a schematic flow sheet is shown in Figure 4. The liquid was pumped from the surge tank through a two-inch pipe which divided into two channels in order to provide flow to each of the two inlets. The transition from the round pipe to the narrow inlets was made by two specially built sections which converged in

UNCLASSIFIED
DWG. 20489

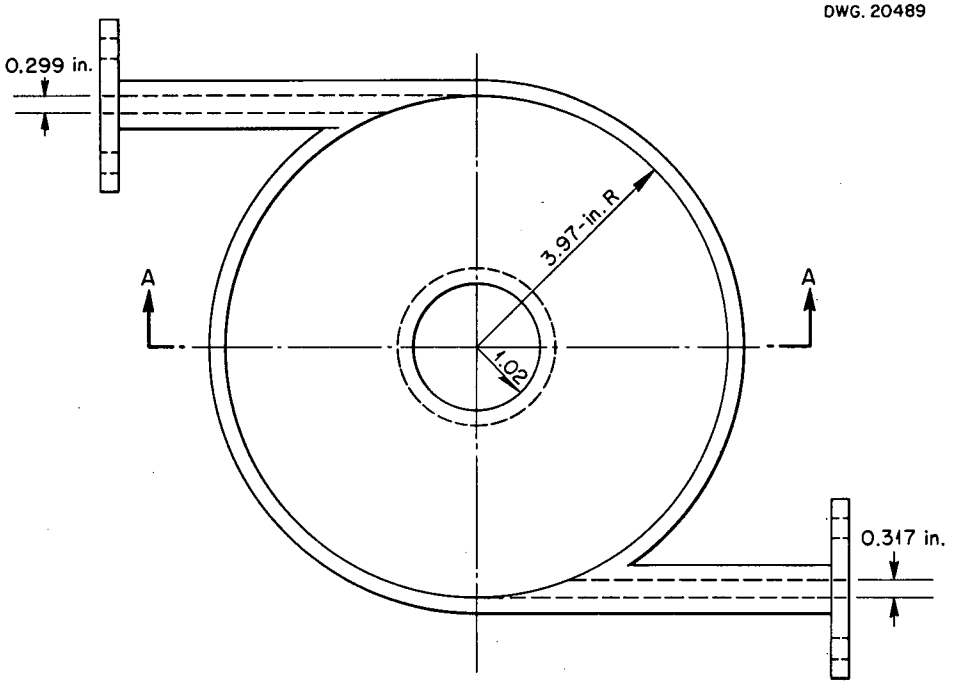

PLAN

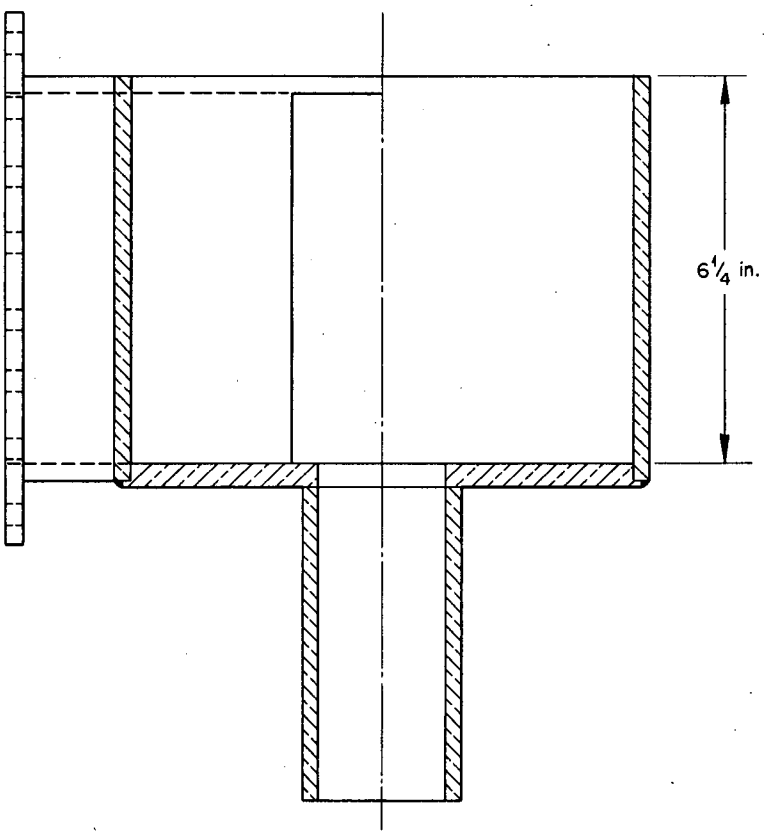

SECTION A-A

Fig. 1. Cylindrical Test Section.

UNCLASSIFIED
DWG. 20490

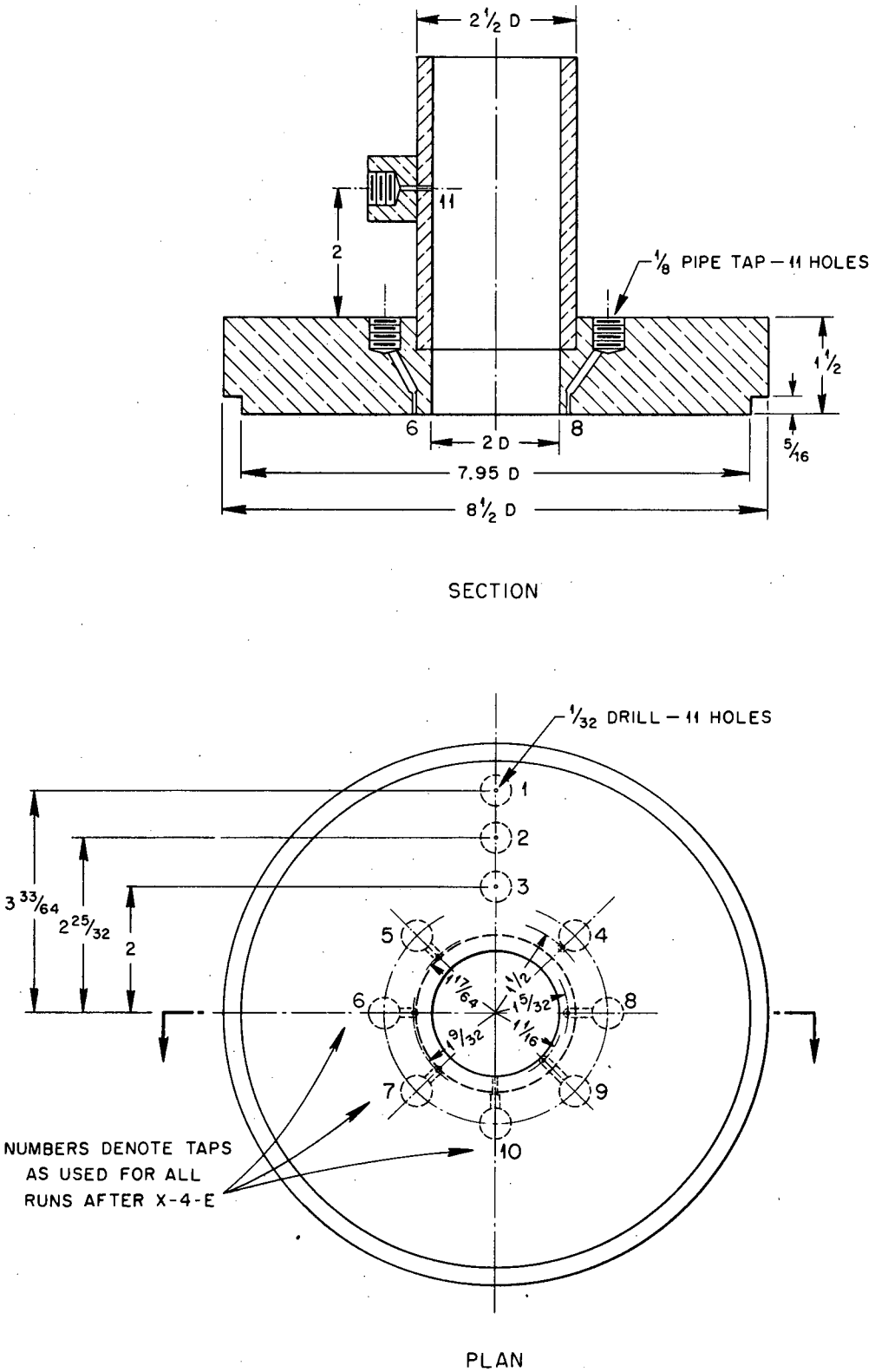

ALL DIMENSIONS ARE IN INCHES

Fig. 2. Top of Cylindrical Test Section.

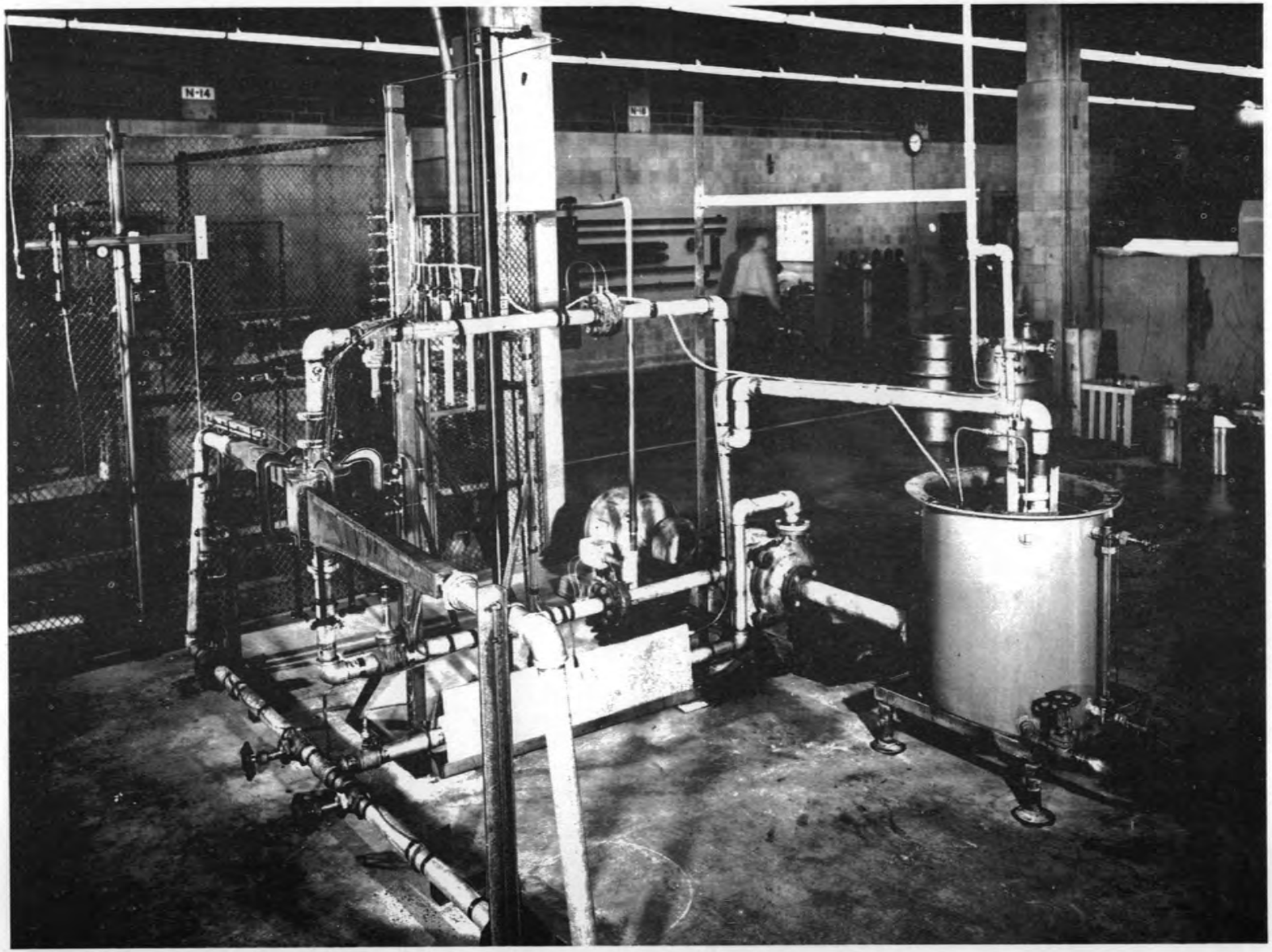

Fig. 3. Photograph of Apparatus.

UNCLASSIFIED
DWG. 20491

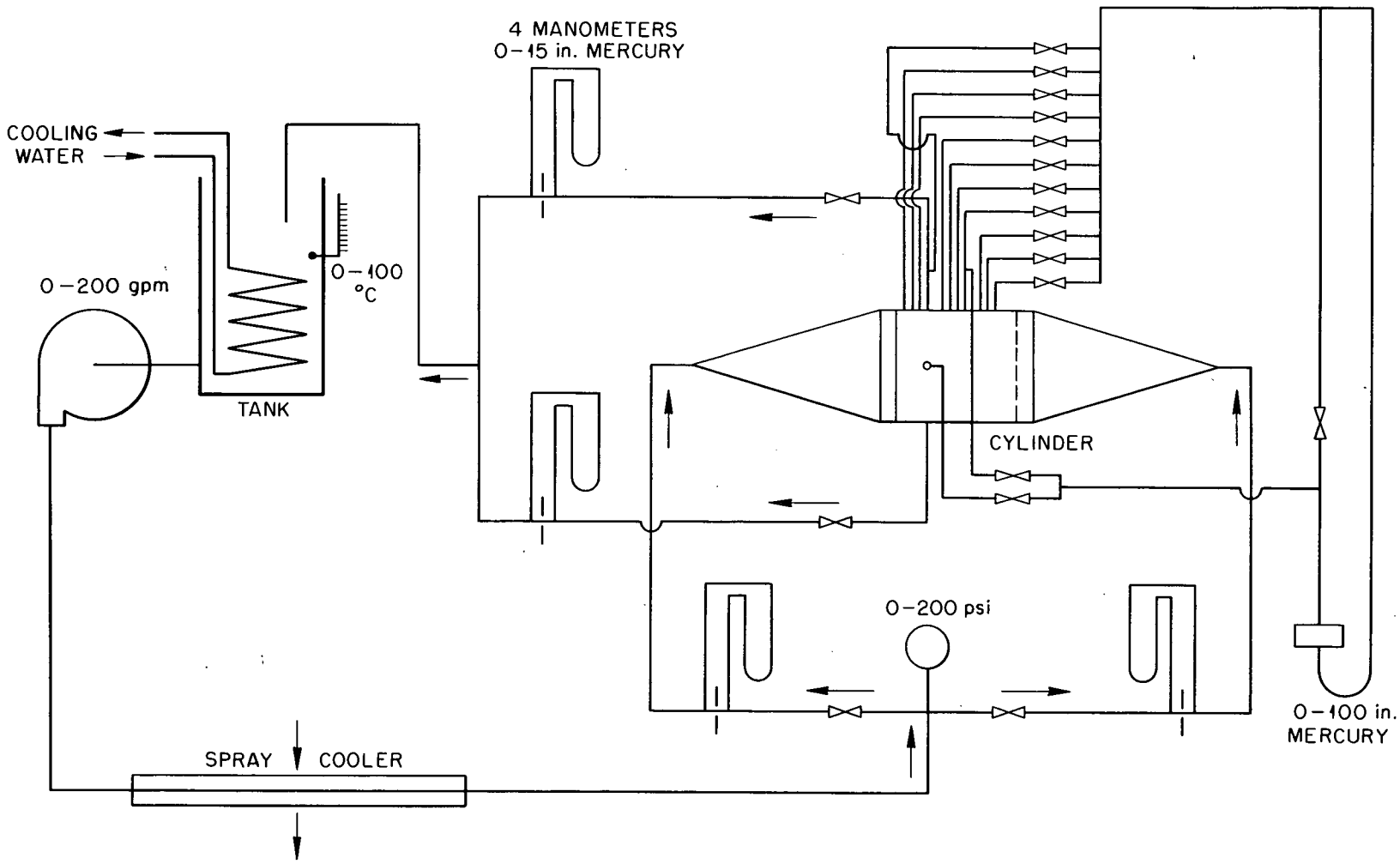

Fig. 4. Flow Diagram for Apparatus.

the width dimension and diverged in the height dimension. The divergence was six degrees total angle, which follows the findings presented by Prandtl and Tietjens (13) with respect to the divergence of channels. It is believed that this arrangement made the entrance of the liquid into the cylinder as uniform as it could practically be made. The swirling liquid made its exit from the cylinder through two outlet channels two inches in diameter at the top and bottom. Flow from the two outlets joined about six feet from the cylinder and was dumped into the surge tank. The flow rate in each inlet and each outlet was metered with a calibrated orifice. Facilities for cooling the system consisted of water cooling coils in the surge tank and a wetted section of piping. Each pressure tap was connected through a small valve to a manifold which was connected to a hundred-inch mercury manometer. The flow rate was controlled by two-inch globe valves in the inlet piping for the cylinder.

CHAPTER V

EXPERIMENTAL PROCEDURE

Two series of experimental runs were made with water in the cylinder which had inlets of widths 0.317 inches and 0.299 inches. The valves were set so that the velocities in the inlets were approximately equal. Attempts were made to obtain data using one inlet, but the data from the taps nearest the outlet were badly scattered, and observation through the plastic cylinder top revealed that the vortex air volume, which was nearly always present, was eccentrically located with respect to the axis of the cylinder. After noting this, all succeeding runs were made with approximately equal flow in the two inlets. The flows in the two outlets were also approximately equal, all flows being metered with calibrated orifices. With the system maintained under a given set of conditions for each run, the pressure measurements at each tap, referred to the outside wall tap, were made in sequence by means of the manifold valve arrangement. The static taps in the upper outlet channel did not exist during the first runs with water. Data are shown in Table XI, Appendix.

Three runs were made with lubricating oil SAE 10 as the fluid. The inlets of widths 0.317 and 0.299 inches were used, and a pressure tap was drilled one sixteenth inch from the lower end of the top outlet before these runs were made. See Table XI, Appendix.

The inlet widths were then changed by soldering in sheet-metal inserts so that the widths were 0.153 inches and 0.141 inches. One more pressure tap was drilled three and one-half inches from the bottom of the top outlet. After these changes were effected, three more runs were made with SAE 10 oil. See Table XI, Appendix.

Using the system as it was during the last three runs with SAE 10 oil, three runs were made with SAE 60 oil. The runs with oil under each condition are fewer than those with water because of the long time (20 minutes) required for the manometer to come to equilibrium as the viscous oil passed through the 0.032 inch pressure taps. The SAE 60 oil was removed from the system and water was run again to get some information about water with the narrow inlets. These data are shown in Table XI, Appendix.

Because the properties of oils with identical SAE numbers can vary widely, the viscosities and densities of the oils used were determined directly using a Westphal type of balance for the density and a Hoeppler viscosimeter for the viscosity. These properties were determined over a temperature range which covered the operating temperatures of the apparatus. Because oil is very difficult to cool, the system operated at temperatures of 60° C. to 75° C. in spite of the one hundred feet of cooling coil placed in the surge tank. The cooling water had an estimated temperature of 10° C. to 20° C. Cooling water was also sprayed on a five-foot section of the piping, but this seemed to have little effect compared with that of the cooling coil.

In an effort to measure directly the tangential velocity and also to study the effect of a probe on the pressure distribution, a Hundstad (9) three-dimensional flow measuring probe was installed on the side of the cylinder. This probe is a special type of pitot tube with the head made of a quarter-inch sphere. This small sphere has three very small pressure taps located on its surface in such a manner that it is a sensing device as well as a velocity measuring device. Velocity readings and pressure distribution readings were taken for four different depths of insertion.

For the final part of the experiment, the pump was disconnected and a one-inch tap-water supply was connected in its place. At the same time the discharge from the cylinder was piped down to the sewer. Dye was introduced into the cylinder for the purpose of measuring residence times in the cylinder. This gave some indication of by-passing along the top and bottom around the main portion of the vortex in the cylinder. See Table XII, Appendix.

CHAPTER VI

RESULTS AND CONCLUSIONS

Effect of Viscosity on the Pressure and Velocity Distribution

Viscosity Effect on β

This study was begun with the intention of evaluating the parameter β, found in the equations of Einstein and Li (4), for liquids with different viscosities. It was supposed that the higher viscosities of liquids such as lubricating oil would prevent the conservation of angular momentum in swirling flow. Furthermore it was hoped that the departure from conservation of angular momentum would be great enough to cause the pressure distribution of the vortex to be markedly different from the pressure distribution of a free vortex. The equation for the static pressure, p, as a function of the radius, r, in a free vortex which is based on the conservation of angular momentum is derived as follows:

$$V = \frac{C}{r} \tag{2}$$

$$d\,p = \frac{\rho}{g_c} \frac{v^2}{r} \, d\,r \tag{28}$$

Substituting (2) in (28)

$$d\,p = \frac{\rho}{g_c} \frac{C^2}{r^3} \, d\,r \tag{29}$$

For the boundary conditions,

$$v = V_R,\ r = R,\ p = P_R, \text{ the solution is}$$

$$P_R - p = \frac{\rho V_R^2}{2\, g_c} \left[\left(\frac{R}{r} \right)^2 - 1 \right] \tag{30}$$

It was found that the experimental data could be represented by equation (30). In using this equation to check the data for its departure from free vortex data, Tables I - V were prepared. It was found that the pressure drop from the cylinder wall to the various radii formed a straight line when plotted against the dimensionless group $\left[\left(\frac{R}{r} \right)^2 - 1 \right]$, as shown in Figures 5 through 9. This can only mean that the correlation indicates the existence of a free vortex pressure distribution for liquids with viscosities as high as 47.2 centipoises. This kind of a pressure distribution indicates that the term $C_1\, r^{1-\beta}$ has negligible values so that the equation,

$$v = C_1\, r^{1-\beta} + C_2\, r^{-1},\ \beta \neq 2 \tag{20}$$

becomes very nearly equivalent to the equation,

$$v = \frac{C}{r} \tag{2}$$

The theoretical values of β as calculated from

$$\beta = \frac{V_o \rho}{2\, \pi\, h \mu} \tag{19}$$

range from about 10 to 10^4 depending upon the fluid and flow conditions. These numbers are rather large, as exponents, and since the momentum losses in the vortex appear to be negligible, it is fitting to assume that the turbulent viscosity values are small

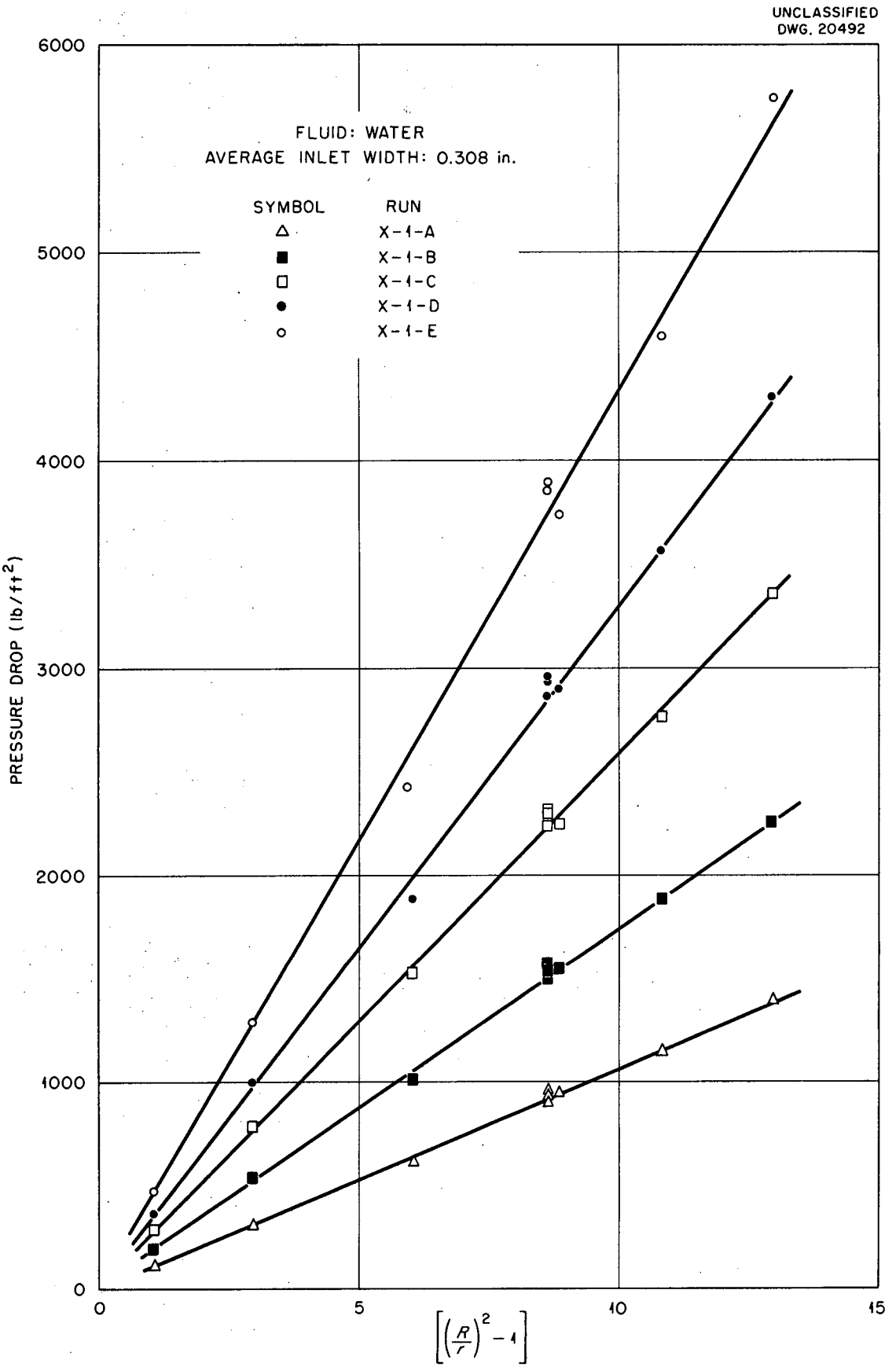

Fig. 5. Pressure Profiles for Water, Using 0.308-in. Inlets.

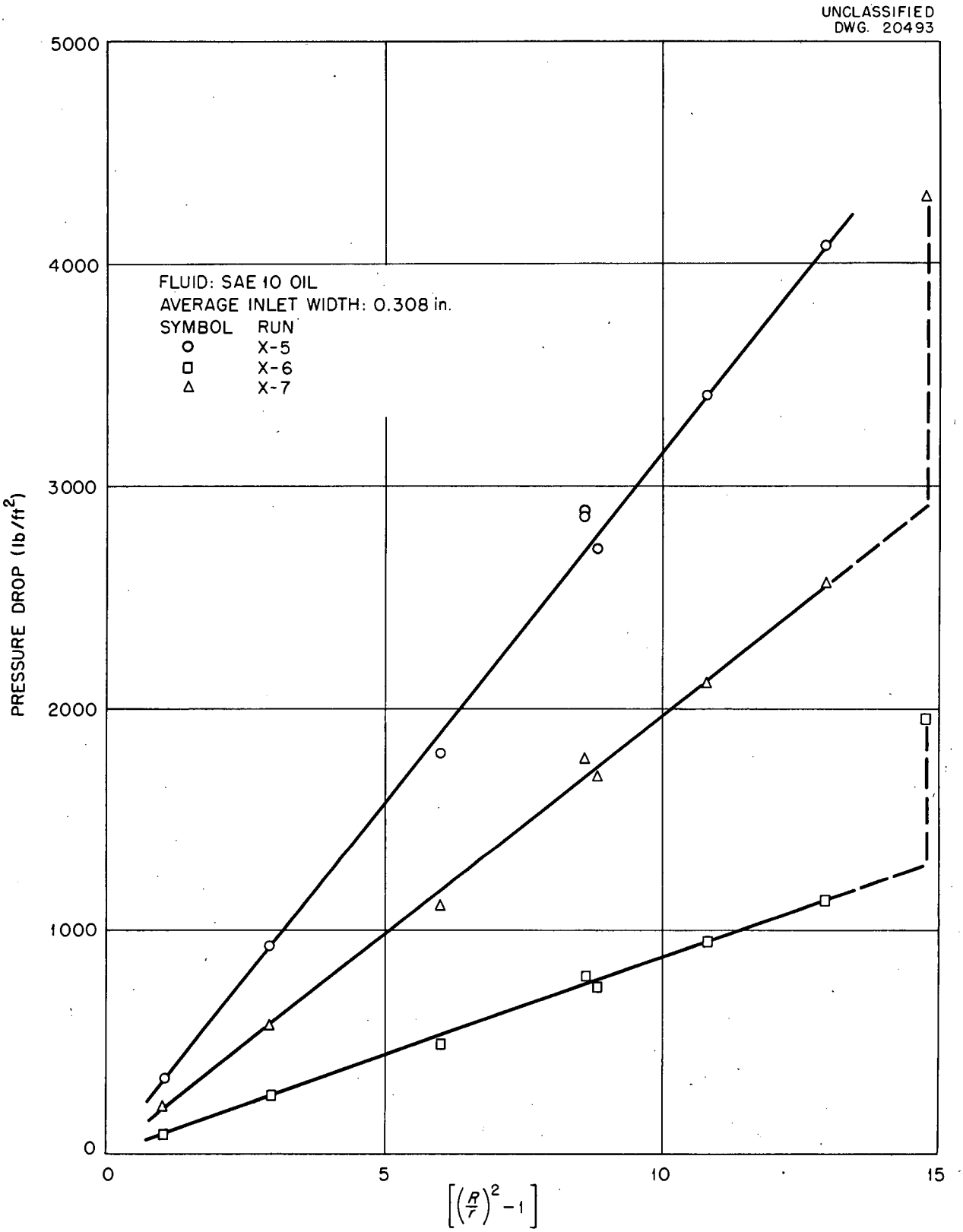

Fig. 6. Pressure Profiles for SAE 10 Oil, Using 0.308-in. Inlets.

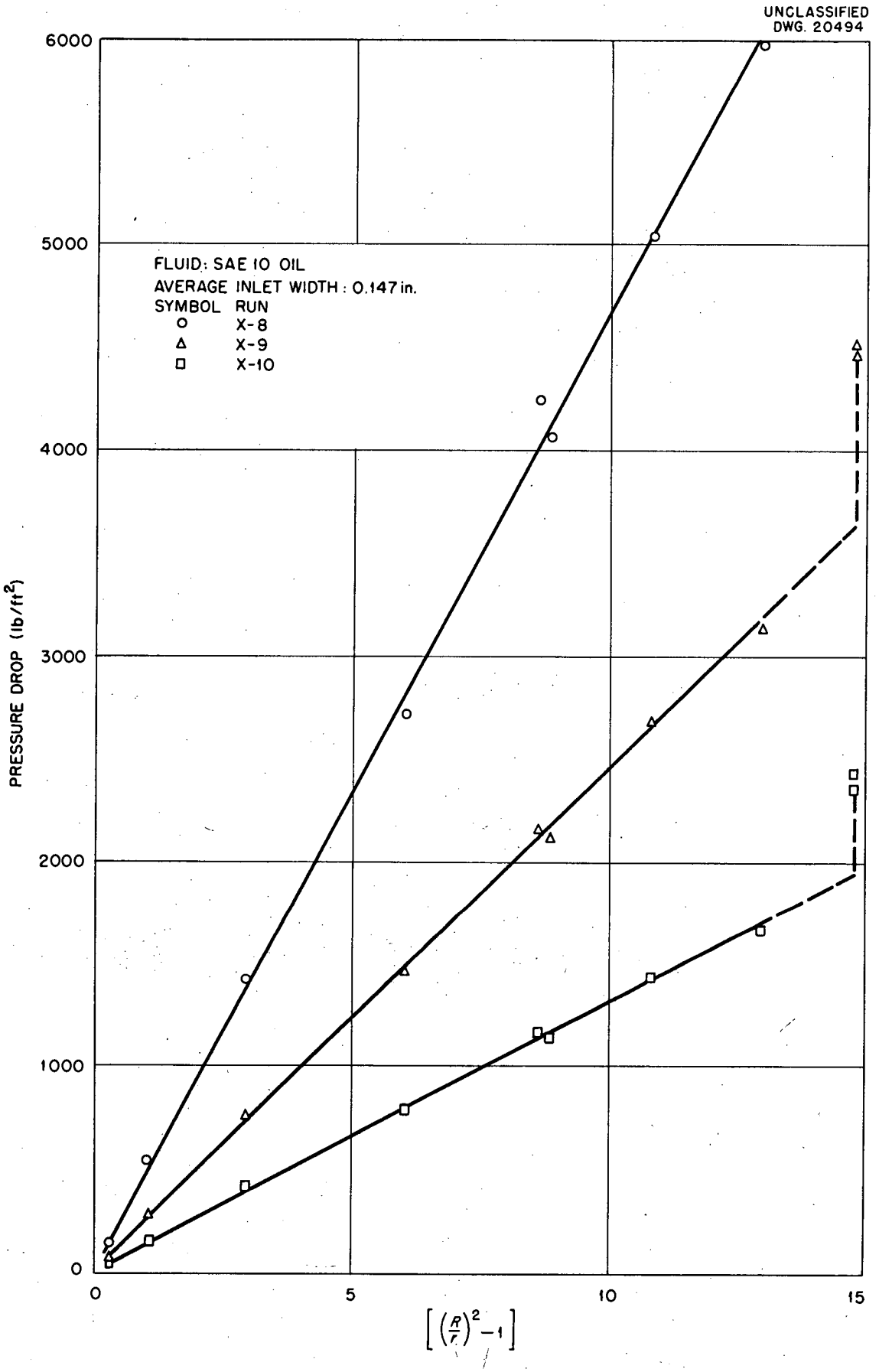

Fig. 7. Pressure Profiles for SAE 10 Oil, Using 0.147-in. Inlets.

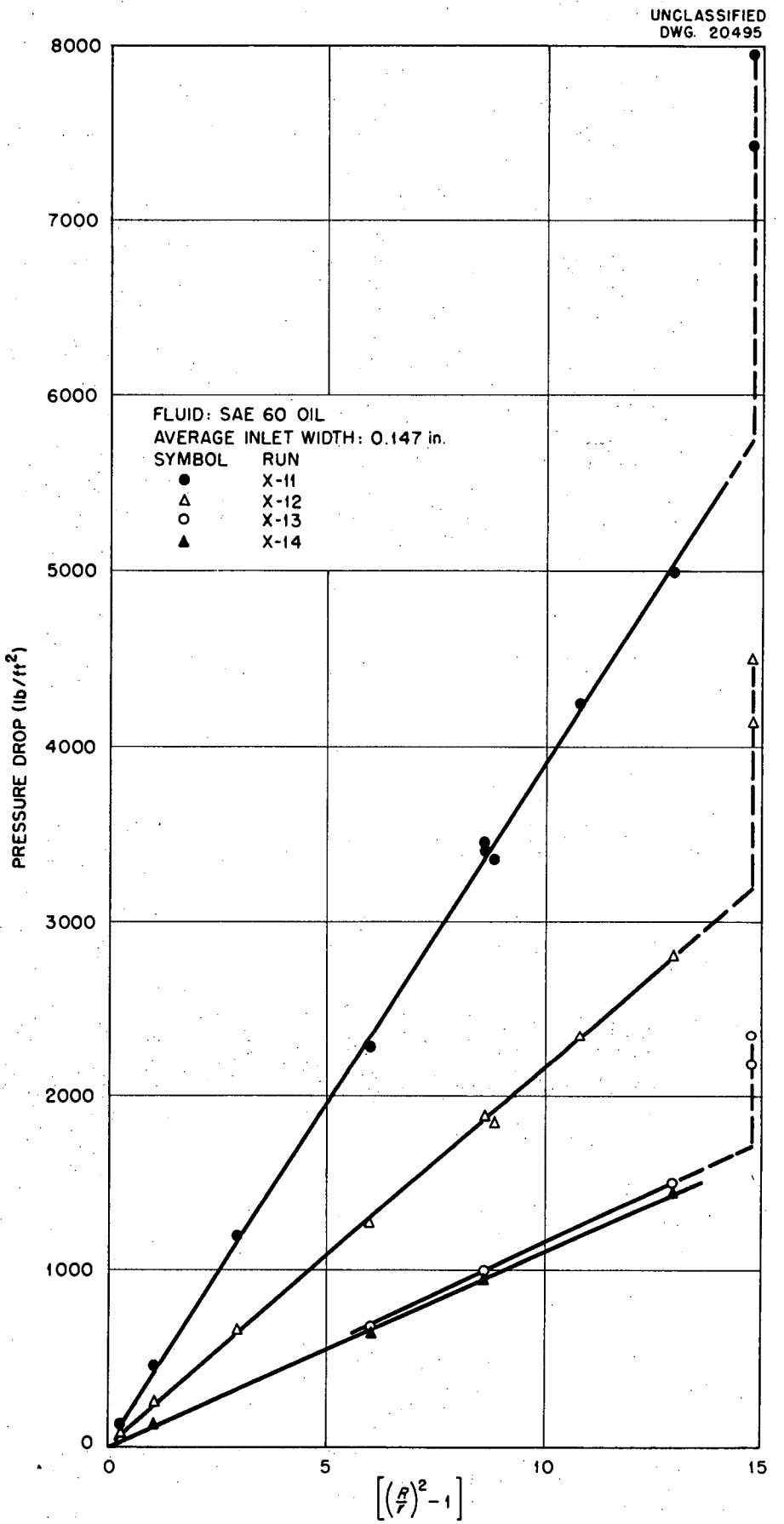

Fig. 8. Pressure Profiles for SAE 60 Oil, Using 0.147-in. Inlets.

UNCLASSIFIED
DWG. 20496

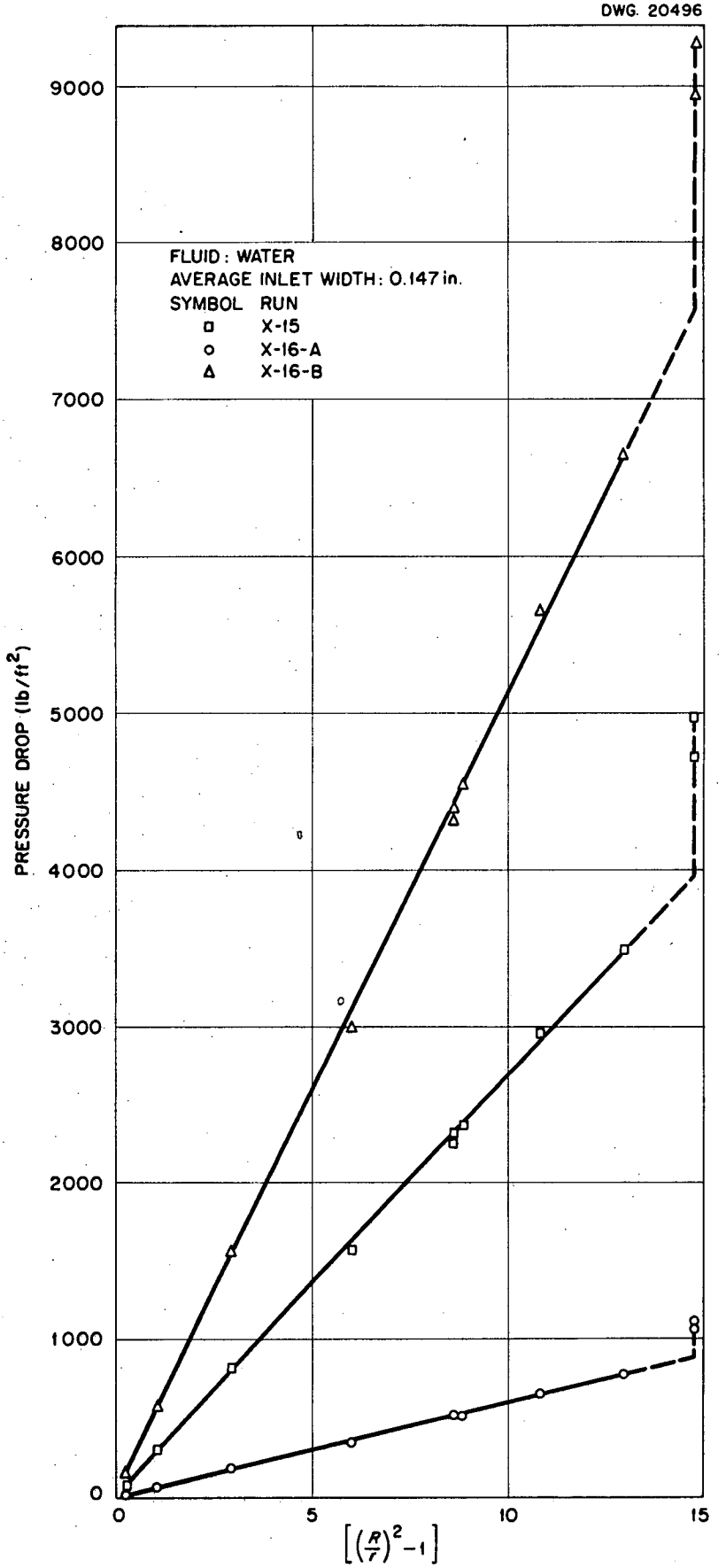

Fig. 9. Pressure Profiles for Water, Using 0.147-in. Inlets.

TABLE I

SUMMARY OF PRESSURE DISTRIBUTION DATA FOR WATER
WITH 0.308-INCH INLETS

Run No.		X-1-A		X-1-B		X-1-C		X-1-D		X-3-A	
Flow Rate (ft^3/sec)		0.257		0.326		0.397		0.456		0.510	
V_i (ft./sec.)		10.02		12.75		15.51		17.79		19.95	
V_R (ft./sec.)		10.4		13.7		16.6		18.7		20.7	
Av. α		1.04		1.07		1.07		1.05		1.04	
Radius (ft)	$\left(\frac{R}{r}\right)^2 - 1$	ΔP lb/ft^2	α^2	ΔP lb/ft^2	α^2	ΔP lb/ft^2	α^2	ΔP lb/ft^2	α^2	ΔP lb/ft^2	α^2
0.293	0.277	13.1	-	49	1.13	78.6	1.23	98.2	1.16	115	1.08
0.232	1.04	105	1.01	196	1.20	282	1.17	364	1.15	432	1.08
0.167	2.95	308	1.04	540	1.17	780	1.14	1000	1.12	1200	1.06
0.125	6.02	615	1.02	1015	1.08	1530	1.10	1890	1.03	2380	1.03
0.106	8.85	950	1.07	1550	1.12	2250	1.10	2900	1.08	3650	1.08
0.107	8.62	970	1.12	1575	1.17	2320	1.16	2960	1.13	3670	1.11
0.107	8.62	960	1.11	1545	1.15	2300	1.15	2940	1.12	3640	1.10
0.107	8.62	934	1.08	1500	1.12	2240	1.12	2870	1.09	3560	1.08
0.0963	10.82	1150	1.06	1890	1.11	2770	1.11	3570	1.08	4500	1.08
0.0886	12.97	1400	1.08	2265	1.12	3360	1.12	4130	1.05	5350	1.08

TABLE I

SUMMARY OF PRESSURE DISTRIBUTION DATA FOR WATER
WITH 0.308-INCH INLETS (continued)

Run No.		X-4-A		X-4-B		X-4-C		X-4-D		X-4-E	
Flow Rate (ft^3/sec)		0.253		0.331		0.387		0.507		0.527	
V_i (ft./sec.)		9.90		12.94		15.16		19.84		20.63	
V_R (ft./sec.)		10.3		14.0		16.2		20.4		21.2	
Av. α		1.04		1.09		1.07		1.04		1.04	
Radius (ft)	$\left(\frac{R}{r}\right)^2 - 1$	ΔP lb/ft^2	α^2	ΔP lb/ft^2	α^2	ΔP lb/ft^2	α^2	ΔP lb/ft^2	α^2	ΔP lb/ft^2	α^2
0.293	0.277	29.5	1.13	52.4	1.17	75.3	1.22	118	1.12	128	1.18
0.232	1.04	108	1.10	203	1.21	275	1.19	439	1.11	475	1.11
0.167	2.95	295	1.06	557	1.19	740	1.13	1195	1.06	1290	1.07
0.125	6.02	564	0.994	1070	1.10	1410	1.06	2270	0.992	2430	0.985
0.106	8.85	848	1.02	1620	1.13	2130	1.09	3440	1.02	3740	1.03
0.107	8.62	890	1.10	1690	1.22	2220	1.16	3560	1.09	3870	1.10
0.107	8.62	904	1.11	1720	1.24	2255	1.18	3610	1.10	3920	1.11
0.107	8.62	887	1.09	1700	1.23	2230	1.17	3560	1.09	3860	1.09
0.0963	10.82	1070	1.05	2050	1.18	2690	1.12	4330	1.05	4600	1.04
0.0886	12.97	1310	1.07	2520	1.21	3310	1.15	5320	1.08	5750	1.08

TABLE II

SUMMARY OF PRESSURE DISTRIBUTION DATA FOR SAE 10 OIL WITH 0.308-INCH INLETS

Run No.		X-5		X-7		X-6	
Flow Rate (ft.^{3}/sec.)		0.460		0.354		0.232	
V_i (ft./sec.)		18.0		13.9		9.10	
V_R (ft./sec.)		19.1		15.0		9.92	
Av. α		1.06		1.08		1.09	
Radius (ft)	$\left(\frac{R}{r}\right)^2 - 1$	ΔP lb/ft^2	α^2	ΔP lb/ft^2	α^2	ΔP lb/ft^2	α^2
0.293	0.277	79.2	1.01	-	-	22.0	1.10
0.232	1.04	333	1.14	204	1.17	89.1	1.19
0.167	2.95	929	1.12	570	1.15	254	1.20
0.125	6.02	1800	1.09	1110	1.10	489	1.13
0.106	8.85	2720	1.09	1690	1.14	741	1.16
0.107	8.62	2860	1.18	1775	1.22	776	1.25
0.107	8.62	2880	1.19	-	-	787	1.27
0.0963	10.82	3410	1.11	2120	1.16	945	1.21
0.0886	12.97	4080	1.12	2570	1.19	1140	1.22
0.0833	14.79	-	-	4300	-	1960	-

TABLE III

SUMMARY OF PRESSURE DISTRIBUTION DATA FOR SAE 10 OIL
WITH 0.147-INCH INLETS

Run No.		X-8		X-9		X-10	
Flow Rate (ft.^{3}/sec.)		0.341		0.240		0.175	
V_i (ft./sec.)		27.9		19.6		14.6	
V_R (ft./sec.)		23.2		16.8		12.3	
Av. α = 0.858							
Radius (ft)	$\left(\frac{R}{r}\right)^2 - 1$	ΔP lb/ft^2	α^2	ΔP lb/ft^2	α^2	ΔP lb/ft^2	α^2
0.293	0.277	145	0.777	76	0.824	40	0.783
0.232	1.04	537	0.766	280	0.809	152	0.792
0.167	2.95	1420	0.714	756	0.770	409	0.752
0.125	6.02	2720	0.671	1460	0.730	785	0.707
0.106	8.85	4070	0.682	2120	0.720	1130	0.692
0.107	8.62	--	--	2160	0.753	1170	0.743
0.107	8.62	4250	0.732	--	--	--	--
0.0963	10.82	5040	0.681	2680	0.745	1430	0.716
0.0886	12.97	5980	0.684	3130	0.725	1675	0.700
0.0833	14.79	--	--	4520	--	2440	--
0.0833	14.79	--	--	4460	--	2360	--

TABLE IV

SUMMARY OF PRESSURE DISTRIBUTION DATA FOR SAE 60 OIL
WITH 0.147-INCH INLETS

Run No.		X-11		X-12		X-13		X-14	
Flow Rate (ft.^{3}/sec.)		0.334		0.258		0.192		0.188	
V_i (ft./sec.)		27.3		21.4		15.7		15.4	
V_R (ft./sec.)		21.2		16.6		12.2		11.9	
Av. α = 0.774									
Radius (ft)	$\left(\frac{R}{r}\right)^2 - 1$	ΔP lb/ft^2	α^2	ΔP lb/ft^2	α^2	ΔP lb/ft^2	α^2	ΔP lb/ft^2	α^2
0.293	0.277	135	0.775	76	0.714	--	--	--	--
0.232	1.04	460	0.702	251	0.628	--	--	125	0.601
0.167	2.95	1195	0.644	656	0.579	--	--	--	--
0.125	6.02	2280	0.602	1270	0.550	676	0.541	640	0.531
0.106	8.85	3360	0.603	1840	0.540	--	--	--	--
0.107	8.62	3410	0.629	1870	0.564	997	0.557	947	0.549
0.107	8.62	3460	0.638	1890	0.570	--	--	--	--
0.0963	10.82	4250	0.623	2340	0.561	--	--	--	--
0.0886	12.97	5000	0.614	2800	0.561	1500	0.558	1430	0.551
0.0833	14.79	7960	--	4500	--	2350	--	--	--
0.0833	14.79	7430	--	4140	--	2180	--	--	--

TABLE V

SUMMARY OF PRESSURE DISTRIBUTION DATA FOR WATER
WITH 0.147-INCH INLETS

Run No.		X-16-B		X-15		X-16-A	
Flow Rate (ft.^{3}/sec.)		0.302		0.217		0.104	
V_i (ft./sec.)		24.6		17.6		8.44	
V_R (ft./sec.)		23.4		16.7		8.01	
Av. α = 0.950							
Radius (ft)	$\left(\frac{R}{r}\right)^2 - 1$	ΔP lb/ft^2	α^2	ΔP lb/ft^2	α^2	ΔP lb/ft^2	α^2
0.293	0.277	157	0.968	85	1.025	19.7	1.035
0.232	1.04	576	0.947	308	0.990	67.5	0.945
0.167	2.95	1560	0.900	818	0.925	178	0.877
0.125	6.02	2990	0.850	1570	0.871	344	0.831
0.106	8.85	4550	0.879	2370	0.895	506	0.834
0.107	8.62	4320	0.857	2250	0.873	512	0.864
0.107	8.62	4400	0.874	2310	0.895	525	0.886
0.0963	10.82	5650	0.891	2960	0.911	656	0.881
0.0886	12.97	6640	0.875	3490	0.900	771	0.866
0.0833	14.79	9290	--	4970	--	1106	--
0.0833	14.79	8960	--	4720	--	1053	--

enough to allow the real values of β to be large. If β is large, then $r^{1-\beta}$ cannot approach zero for values of $r < 1$. The only way, then, for $C_1 r^{1-\beta}$ to become negligible (or zero) is for C_1 to be very small (or zero). Kassner's theory of constant moment of momentum along the radius, reviewed on page 8 , says that no matter what value the viscosity has, the free vortex velocity distribution is to be expected. This may possibly explain why C_1 appears to be very small or zero. If this is the case, it cannot be discerned from these experiments because the frictional effect of the peripheral cylinder wall has not been isolated from the internal frictional effect. If the friction losses in the interior of the vortex were larger this might be possible.

Effect of Viscosity on the Peripheral Velocity

Since viscosity has a negligible effect upon the shape of the pressure profile of the vortices formed, as is reflected in the agreement of the experimental data with the theoretical equation of inviscid flow, it is only logical to look for other manifestations of a viscous effect. For one cylinder geometry (that with the 0.147 inch inlets) this effect can be evaluated. From equation (30) and the curves in Figures 7, 8, and 9, the effective peripheral velocity, V_R, of each specific vortex can be computed. From each known flow rate the corresponding average inlet velocity, V_i, can be computed. The relationship between these two factors for the three liquids used in the same cylinder geometry, is shown in Figure 10. Notice that V_R is a straight-line function of V_i, but the slope decreases with increasing viscosity.

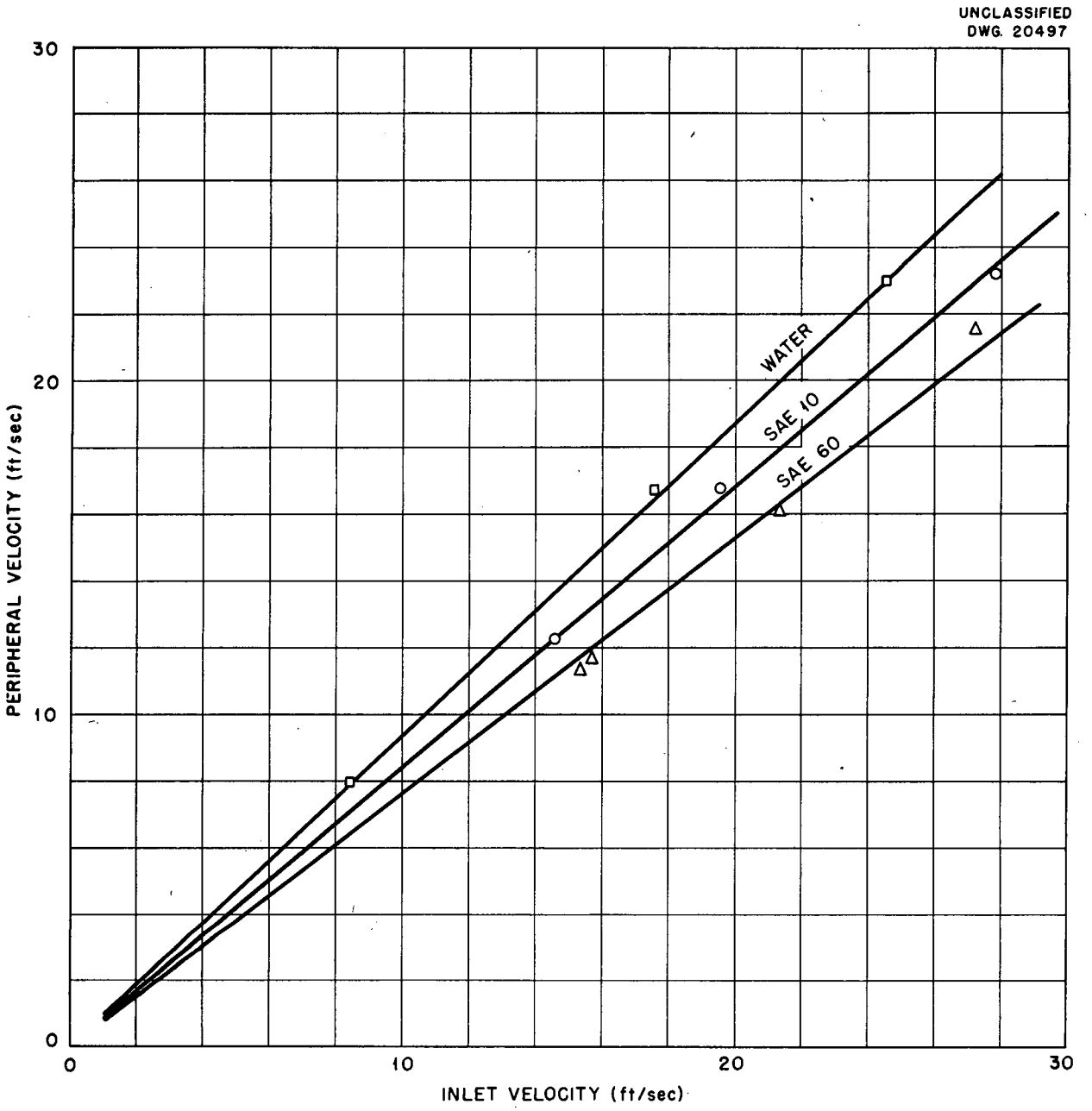

Fig. 10. Effect of Viscosity on the Ratio of Peripheral Velocity to Inlet Velocity.

$$V_R = \alpha V_i \tag{31}$$

In order to determine the best mean value of α for each fluid, the slopes of the curves in Figure 10 were not relied upon. Instead αV_i was substituted into equation (30), and this equation was solved for α^2.

$$\alpha^2 = \frac{2g_c}{V_i^2 \rho} \quad \frac{\Delta P}{\left[\left(\frac{R}{r}\right)^2 - 1\right]} \tag{32}$$

$$\Delta P = P_R - p$$

For each fluid the values of α^2, which are shown in Tables III - V, were averaged and the square root of the average was extracted, giving a value of α to be associated with the particular cylinder geometry used. The variation of α with viscosity is presented in Table VI.

TABLE VI

THE VARIATION OF α WITH VISCOSITY

Viscosity, cp.	α
0.854	0.950
12.3	0.858
47.2	0.774

Based on the evidence from these experiments, it appears that the parameter β is quite insensitive to viscosity. On the other hand the parameter α, which seems to show the effect of drag on the fluid at the cylinder wall, shows a measurable dependence upon viscosity.

The low values of β obtained by Einstein and Li (4) and by Garber and Peebles (6) are still not explained. However, the evidence reported here eliminates turbulence as an explanation. The high turbulence observed in the cylinder failed to yield a value of β small enough to be measurable. The explanation may lie somewhere in the simplifying assumptions used by these authors about the nature of the flow in the containers. It will presently be shown that the assumption of uniform radial velocity is not true, although it may still be a practical assumption.

Effect of the Radial Velocity Variations on the Flow Pattern

It will be remembered that Einstein and Li (4) assumed in their development that for a given radius the radial velocity was constant. For flow in a cylinder such as the one used in this investigation, it was doubtful if this assumption would hold. The reasoning behind this is that the top and bottom surfaces of the cylinder exert a drag on the swirling liquid and retard the tangential component of velocity near the top and bottom. This is very similar to the secondary flow in a curved section of pipe described in the work edited by Goldstein (7). In the pipe there

is flow toward the inside of the horizontally curved channel at the top and bottom, while there is flow toward the outside of the curved channel in the central region. In the cylinder the same principle governs the flow, but instead of having outward flow in the central region of the channel, the radial velocity is lower than it is near the top and bottom. The retardation of the tangential velocity near the top and bottom tends to lower the centrifugal pressure exerted by the swirling in these boundary regions, but the system maintains the equilibrium pressure condition at a given radius by increasing the radial velocity. A form of Bernoulli's equation can be used to illustrate.

$$\frac{V^2}{2g} + \frac{p}{\rho} = \text{a constant} \tag{33}$$

V is the resultant magnitude of the velocity at a point, and p is the static pressure at the same point. Here it is maintained that this equation holds for any vertical line in the interior regions of the vortex that lie outside of the outlet radius, and the mechanism which can cause this to be true will be explained.

The resultant V is composed of two components, u and v.

$$V = \sqrt{u^2 + v^2} \tag{34}$$

Substituting in equation (33),

$$\frac{u^2 + v^2}{2g} + \frac{p}{\rho} = \text{a constant} \tag{35}$$

Now pass an imaginary vertical line, parallel to the axis, through the vortex at a location denoted by some radius less than the cylinder radius and greater than the outlet radius. At a point on this

line well away from the top and bottom boundaries, v has values greater than it does at points near the top and bottom boundaries, due to the drag of these boundaries. In order for p to remain constant along the line, u must be greater near the top and bottom than it is in the region in between. This would mean that there is a by-passing flow near the top and bottom, and that the residence time of liquid in the interior regions is longer than the average theoretical residence time, based on slug flow, for liquid in the cylinder. This theory was checked by measuring the time required to remove coloring matter from the cylinder at known flow rates. The result of this is in Figure 11 and Table VII. For comparison the average theoretical residence time, based on slug flow through the entire cylinder volume, is also shown. The straight lines show that the relative residence times are independent of flow rate, and that the maximum residence time of liquid in the interior part of the vortex is 3.86 times as great as the average residence time, based on slug flow. This by-passing effect is an explanation for the fact that the pressure taps give the free vortex pressure distribution although the drag of the top and bottom boundaries bring into existence boundary layers near them which do not contain the free vortex velocity distribution. In short, a free vortex in the interior determines the pressure distribution; increased radial velocities near the top and bottom maintain a constant pressure at a given radius regardless of vertical location.

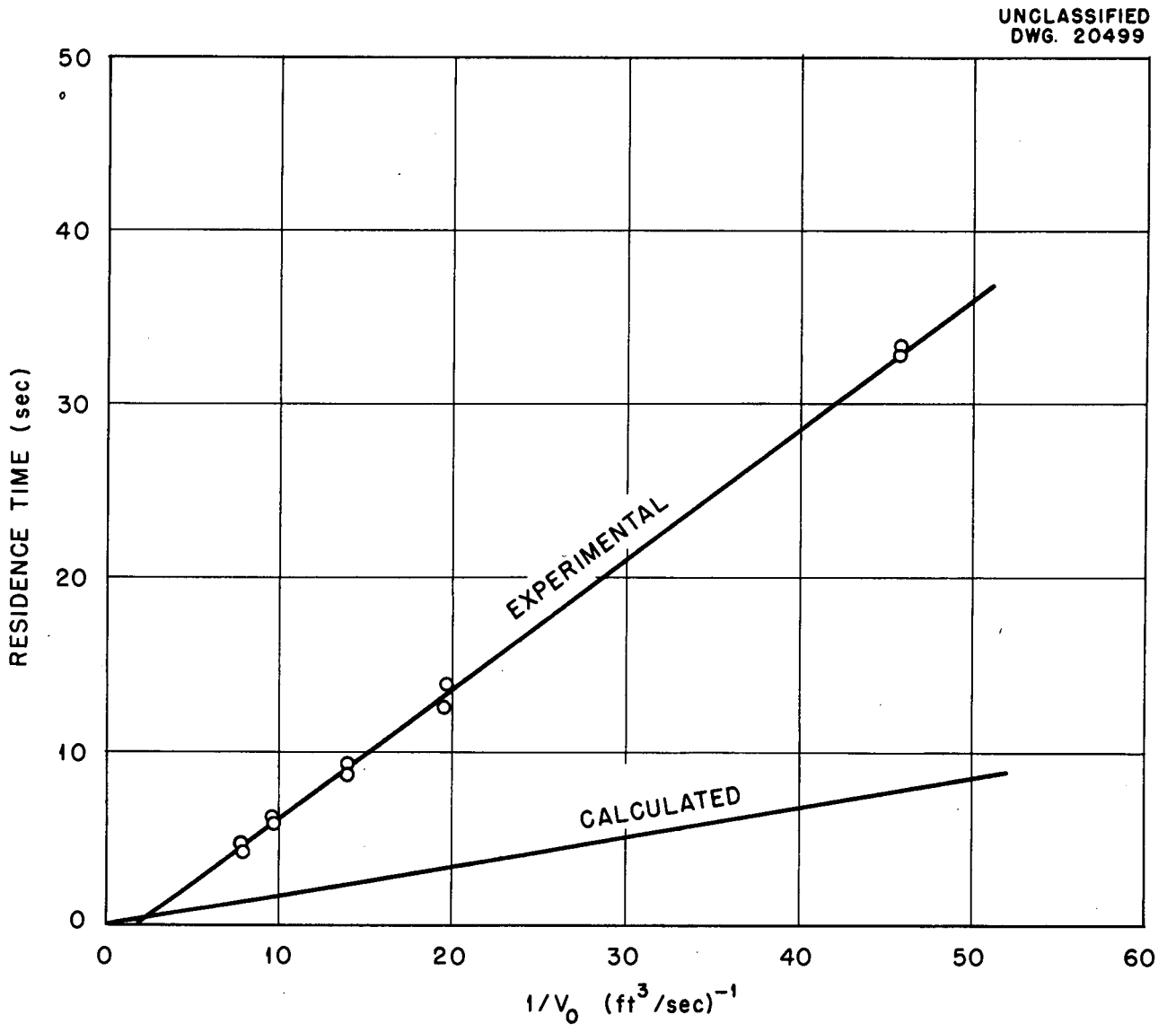

Fig. 11. Residence Times for Water in Cylinder.

TABLE VII

RESIDENCE TIMES FOR WATER IN THE CYLINDER

Run	Vo Flow (ft.^{3}/sec)	$\frac{1}{Vo}$	Measured Residence Time (sec.)	Calculated Residence Time (sec.)
1	0.0219	45.7	33.4	7.84
2	0.0219	45.7	32.8	7.84
3	0.0218	45.9	33.2	7.88
10	0.0510	19.6	13.8	3.37
11	0.0513	19.5	12.5	3.35
12	0.0510	19.6	12.6	3.37
13	0.0719	13.9	8.7	2.39
14	0.0719	13.9	9.3	2.39
15	0.0719	13.9	8.8	2.39
7	0.103	9.73	5.9	1.67
8	0.104	9.65	6.1	1.66
9	0.103	9.70	5.9	1.67
4	0.127	7.85	4.2	1.35
5	0.128	7.80	4.6	1.34
6	0.129	7.75	4.5	1.33

Determination of Tangential Velocities Using a Horizontal Pitot Probe

As was described in Chapter V, measurements of the tangential velocity using a Hundstad pitometer were made. The Hundstad three-dimensional flow measuring probe had a one-fourth inch diameter spherical head on the end of a one-fourth inch diameter tube. An attempt was made to measure the velocity at different depths of insertion along a cylinder radius. Values were actually obtained, but there is evidence that they are not the velocities that would exist without the probe. This evidence consists of the comparison of the static pressure profiles for the various depths of insertion, shown graphically in Figure 12. The flow data are given in Table VIII. Note that the most shallow insertions gave the greatest slope in spite of the fact that they were associated with the lowest flow rates in each of the two cases. Note also the scattering of the static pressure data for the greatest depths of insertion. Apparently the probe disturbed the flow pattern to such an extent that velocity data are questionable if one attempts to associate a velocity probe traverse with a single vortex. In Figure 13 are shown velocity probe traverses for two different conditions. Assuming that each set of points is associated with a single vortex, it appears that each vortex is markedly different from a free vortex; i.e., the slope of each solid line is 0.70. (a free vortex has the slope, 1.0). However, this is very misleading. The curves in Figure 12 are evidence that

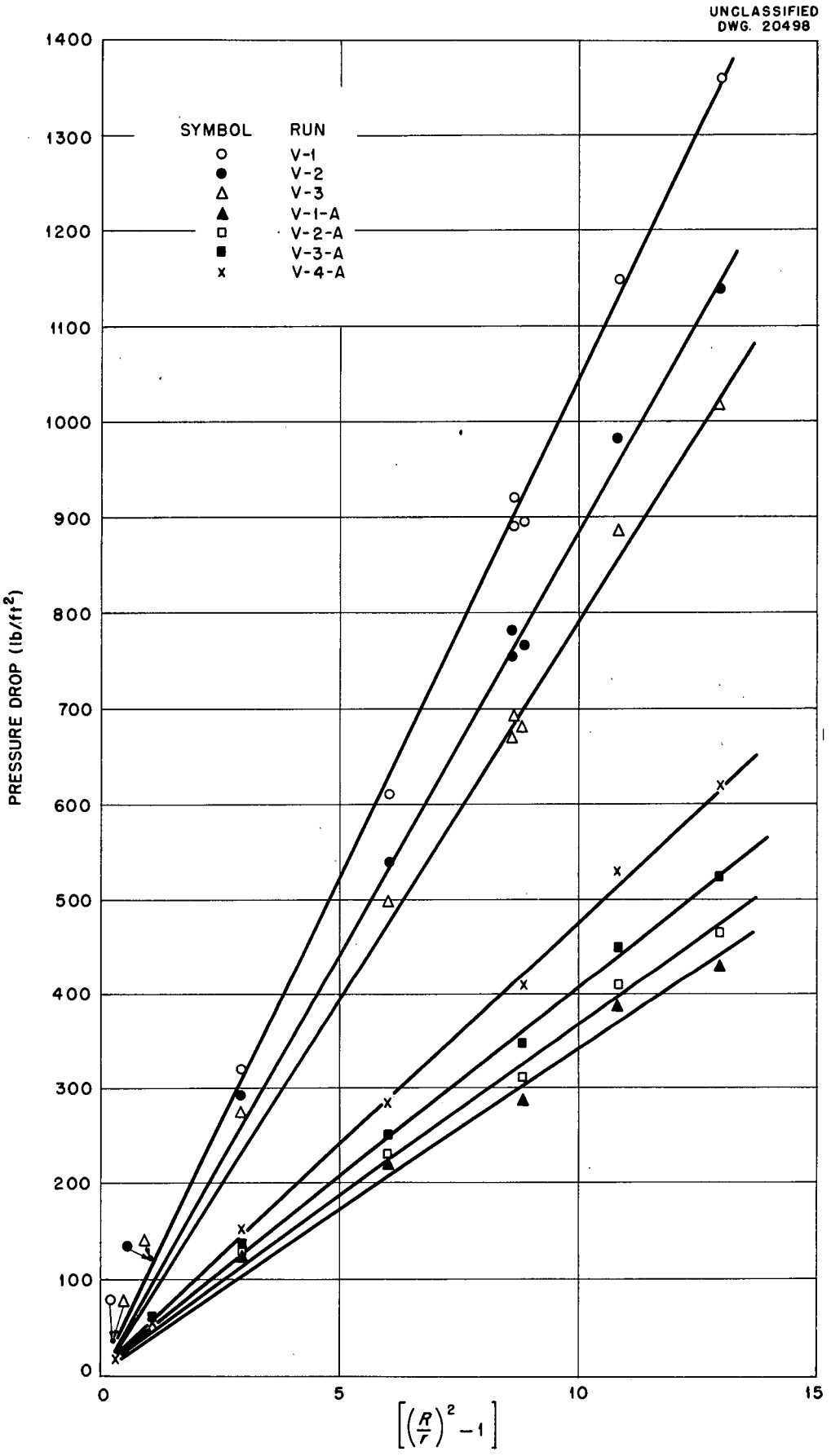

Fig. 12. Effect of Probe on Pressure Distribution.

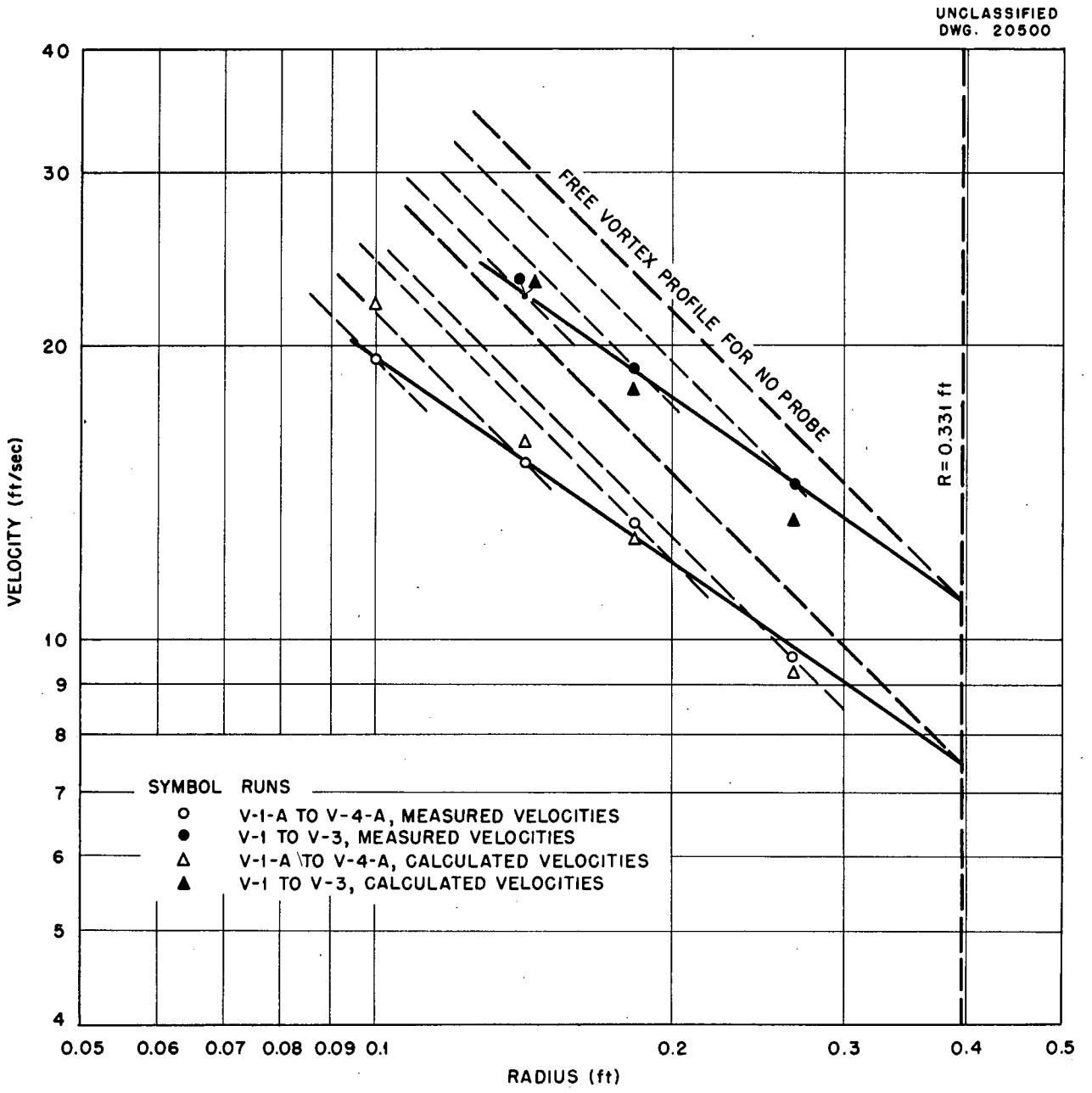

Fig. 13. Effect of Probe on Velocity Profile.

TABLE VIII

PRESSURE DISTRIBUTIONS FOR VARIOUS PROBE INSERTIONS

Run No.		V-1-A		V-2-A		V-3-A		V-4-A	
Flow Rate(ft^3/sec)		0.110		0.100		0.099		0.097	
Velocity at Probe Head (ft./sec.)		19.4		15.1		13.1		9.6	
V_i (ft./sec.)		8.88		8.12		8.00		7.86	
(α V_i)(R/r) at Probe Head(ft/sec)		22.0		15.9		12.7		9.19	
Probe Head Position Radius (ft.)		0.100		0.142		0.183		0.266	
α		0.750		0.841		0.881		0.940	
Radius (ft)	$\left(\frac{R}{r}\right)^2 - 1$	ΔP lb/ft^2	α^2	ΔP lb/ft^2	α^2	ΔP lb/ft^2	α^2	ΔP lb/ft^2	α^2
0.293	0.277	18.3	0.867	19.6	1.111	19.6	1.146	19.6	1.185
0.232	1.04	55.6	0.702	55.6	0.840	57	0.888	59	0.950
0.167	2.95	124	0.552	128	0.681	137	0.752	151	0.858
0.125	6.02	220	0.479	232	0.606	252	0.678	284	0.790
0.106	8.85	288	0.427	314	0.557	350	0.641	410	0.776
0.0963	10.82	390	0.475	410	0.594	451	0.675	530	0.820
0.0886	12.97	432	0.437	468	0.566	527	0.658	621	0.802

Run No.		V-1		V-2		V-3	
Flow Rate(ft^3/sec)		0.135		0.135		0.130	
Velocity at Probe Head (ft./sec.)		14.3		18.8		22.4	
V_i (ft./sec.)		11.0		11.0		10.6	
(α V_i)(R/r) at Probe Head(ft/sec)		13.2		18.0		22.3	
Probe Head Position Radius (ft.)		0.266		0.183		0.142	
α		0.965		0.903		0.904	
Radius (ft)	$\left(\frac{R}{r}\right)^2 - 1$	ΔP lb/ft^2	α^2	ΔP lb/ft^2	α^2	ΔP lb/ft^2	α^2
0.293	0.277	36	1.111	36	1.111	36	1.198
0.232	1.04	121	0.996	118	0.971	118	1.045
0.167	2.95	320	0.929	292	0.848	275	0.859
0.125	6.02	611	0.869	540	0.768	498	0.763
0.106	8.85	897	0.867	767	0.741	681	0.709
0.107	8.62	891	0.884	753	0.750	672	0.719
0.107	8.62	920	0.914	783	0.787	692	0.740
0.0963	10.82	1150	0.920	982	0.777	888	0.756
0.886	12.97	1360	0.896	1140	0.752	1020	0.735

the vortices involved were very nearly free vortices. Each time the probe depth was changed a new vortex was created even though the flow was nearly constant for the given traverse, and each measured velocity shown in Figure 13 was actually associated with a different vortex. The velocity distribution that should rightfully be associated with each point is shown by the broken lines in Figure 13. The calculated velocities on Figure 13 are shown for comparison with the measured velocities. The calculation was carried out by first determining α for each individual probe setting, using the method described on page 38; then substituting this value in the equation,

$$v = \alpha V_i \frac{R}{r} \tag{36}$$

In the light of the preceding analysis the velocity data of Shepherd and Lapple (16, 17) for cyclones should be reexamined. It is possible that they collected data for a series of vortices which gave them a slope of 0.5 and caused equation (1) with $n = 0.5$ to fit their data. The main point to be emphasized here is that velocity data obtained with probes inserted perpendicular to the vortex axis are misleading and should not be considered as accurate data for a single vortex. In order to entirely clear up this point, pressure distributions with different depths of probe insertions should be obtained for gases in swirling flow.

Relation of the Total Pressure Drop Across the Cylinder to the Radial Pressure Profile

The pressure drop from the cylinder wall to the outlet channel presents a perplexing problem. On Figures 6 through 9 there are points, where the abscissa has the value 14.79, that lie well above their associated pressure distribution curves. If a pressure profile for that portion of the cylinder which lies outside of the outlet radius be extrapolated to the abscissa 14.79, which corresponds to the outlet radius, the difference between this point of extrapolation and the measured pressure drop is about twenty to fifty per cent of the value of ΔP at the extrapolated point. This extra pressure drop may be something as simple as a contraction loss, but it is believed to be considerably more complicated. The centrifugal forces acting on the liquid in the outlet channel cause most of the exit liquid to flow through an annular cross section. If the thickness of the annular cross section were known, one could test the contraction loss theory with a calculation, but that lies outside this investigation. The behavior in the outlet region is the subject of another investigation now under way at the University of Tennessee Department of Chemical Engineering, and will not be further discussed here.

Conclusions

The results previously discussed in this chapter lead to the conclusions that follow.

The parameter β was not visibly affected by changing the viscosity over a range of three orders of magnitude. However, it was observed that the parameter α is a function of viscosity. The function was not determined, since this could lead to another investigation on a scale equal to that of this report.

The radial velocity was greater near the top and bottom boundaries of the cylinder, but the pressure distribution was still that of a free vortex.

The velocity probe inserted normally to the vortex axis did not give accurate velocity values because the pressure distribution, and, hence, the velocity distribution, was altered by changes in the depth of insertion.

There are pressure losses in the outlet channels that appear to be of sufficient complexity to justify a separate experimental investigation.

LIST OF REFERENCES

AND

BIBLIOGRAPHY

LIST OF REFERENCES

1. Alexander, R. M., "Fundamentals of Cyclone Design and Operation" Australasian Inst. Min. & Met. Proc. 152-153, 203-208 (1949)

2. Daugherty, R. L., Hydraulics, New York, McGraw-Hill, 1937

3. Driessen, M. G., "The Use of Hydraulic Cyclones in Thickeners and Washers in Modern Coal Preparation" Trans. Am. Inst. Min. & Met. 177, 240 (1948); Coal Tech. TP2135 (1947)

4. Einstein, H. A. and Li, H., "Steady Vortex Flow in a Real Fluid," Heat Transfer and Fluid Mechanics Institute, Stanford University, pp. 33-43, 1951

5. Fulton, C. D., "Ranques Tube" Refrig. Eng. 58, 473-479 (1950)

6. Garber, H. J. and Peebles, F. N., "Nature of Liquid Flow Within a Spherical Container," Second Quarterly Report under Contract No. W7405-eng-26, 5-370, Knoxville, Tennessee, Dept. of Chemical Engineering of the University of Tennessee (1951)

7. Goldstein, S., Modern Developments in Fluid Dynamics, Vol. I, Oxford University Press, 1938, p. 84

8. Green, S. L., Hydro-and Aero-Dynamics, Second Edition, Isaac Pitman and Sons, 1947, pp. 140-141

9. Hundstad, R. L., "Three Dimensional Flow Measuring Probe" Proc. Midwestern Conference on Fluid Dynamics, Second Conference (1952)

10. Kassner, R. and Knoernschild, E., "Friction Laws and Energy Transfer in Circular Flow" Technical Report No. F-TR-2198-ND, G-S-USAF, Wright-Patterson Air Force Base No. 78, Project No. LP-259, Air Material Command

11. Kelsall, D. F., "Motion of Solid Particles in a Hydraulic Cyclone" Inst. Chem. Eng. (London) 30, 87-108 (1952)

12. Lissman, M. A., "Mechanical Methods of Dust Collection" Chem. and Met. Eng. 37, 630-634 (1930)

13. Prandtl, L. and Tietjens, O. G., Applied Hydro and Aeromechanics, First Edition, New York, McGraw-Hill, 1934

14. Russell, G. E., Hydraulics, Fifth Edition, New York, Holt, 1949, pp. 444-445

15. Saito, N. and Ito, K., "On the Velocity Distribution in Simple Vortex" Geophysical Magazine (Tokyo) 22, 283-288 (1951)

16. Shepherd, C. B. and Lapple, C. E., "Flow Pattern and Pressure Drop in Cyclone Dust Collectors" Ind. Eng. Chem. 31, 972 (1939)

17. Shepherd, C. B. and Lapple, C. E., "Flow Pattern and Pressure Drop in Cyclone Dust Collectors" Ind. Eng. Chem. 32, 1246 (1940)

18. Stairmand, C. J., "Pressure Drop in Cyclone Separators" Engineering 168, 409 (1949)

19. Taylor, G. I., "Distribution of Velocity and Temperature between Concentric Rotating Cylinders" Proc. Roy. Soc., A. 151, 494-512 (1935)

20. Taylor, G. I., "The Transport of Vorticity and Heat through Fluids in Turbulent Motion" Proc. Roy. Soc., A, 135, 685-702 (1932)

21. Wattendorf, F. L., "A Study of the Effect of Curvature on Fully Developed Turbulent Flow" Proc. Roy. Soc., A, 148, 565-598 (1935)

BIBLIOGRAPHY

Ambler, C. M., "New Developments in Centrifuge Applications" Chem. Eng. Prog. 44, 405-410 (1948)

Arthur, P. D., "Operation and Theory of the Hilsch Tube." University of Maryland Thesis (M.S.) 1948

Binnie, A. M. and Hookings, G. A., "Laboratory Experiments on Whirlpools" Proc. Roy. Soc., A, 194, 398-415 (1948)

Binnie, A. M. and Harris, D. P., "The Application of Boundary Layer Theory to Swirling Liquid Flow through a Nozzle" Quart. Jr. Mech. and Applied Math., 3, 89-106 (1950)

Binnie, A. M. and Davidson, J. F., "The Flow under Gravity of a Swirling Liquid through an Orifice Plate" Proc. Roy. Soc. A, 199, 443-457 (1949)

Binnie, A. M., "The Passage of a Perfect Fluid through a Critical Cross-section or 'Throat'" Proc. Roy. Soc. A, 197, 545-555 (1949)

Binnie, A. M., "The Theory of Waves Travelling on the Core in a Swirling Liquid" Proc. Roy. Soc., A, 205, 530-540 (1951)

Curley, W. and MacGee, R., "Bibliography of the Vortex Tube" Refrig. Eng. 59, 166 (1951)

Dahlstrom, D. A. and Maeser, R. W., "Cyclone Elimination of Contaminating Solids from Process Water" Coal Tech. TP2471 (1948); Trans. Am. Inst. Min. & Met. 177, 277 (1948)

Dahlstrom, D. A., "Cyclone Operating Factors and Capacities on Coal and Refuse Slurries" Trans. Am. Inst. Min. & Met. 184, 331-334 (1949); Min. Eng. TP2633P (1949)

Dahlstrom, D. A., "High Efficiency Desliming by the Use of Hydraulic Water Additions to the Liquid-solid Cyclone" Min. Eng. 4, 788-793 (1952)

Dahlstrom, D. A., "High Speed Classification and Desliming with the Liquid-solid Cyclone" Trans. Am. Inst. Min. & Met. 190, 153 (1951)

Drinker, P. and Hatch, T., Industrial Dust, New York, McGraw-Hill, 1936

Eisenschitz, E., "Recent Theories of Transport Processes in Liquids" Nature (London) 167, 216-220 (1951)

Fern, K. A., "The Cyclone as a Separating Tool in Mineral Dressing" Trans. Inst. Chem. Engrs. 30, 82-86 (1952)

Fitch, E. B. and Johnson, E. C., "Controlling Separation in Liquid-solid Cyclones" Chem. Eng. 59, 172-173 (1952)

Hagerty, W. W. and Yeagle, R. A., "Photoviscosity of Glycerine Proves Useful Tool in Flow Studies" Civil Eng. 21, 702-704 (1951)

Hilsch, R., "Use of the Expansion of Gases in a Centrifugal Field as a Cooling Process" R. of Scientific Instruments 18, 108-113 (1947)

Hooper, F. C. and Juhasy, J. S., "Electric Dew Point Meter Cooled by the Vortex Tube" Refrig. Eng. 60, 1196-1197 (1952)

Kennedy, G. H. and Criner, H. E., "Application of Cyclone Thickeners to Preparation Plant Water Circuits" Min. Eng. TP2991 (1951); Trans. Am. Inst. Min. & Met. 190, 259 (1951)

Krebs, K., "The Centriclone Classifier" Min. Cong. Journal 38, 48-49 (1952)

Lapple, C. E., "Isothermal and Adiabatic Flow of Compressible Fluids" Trans. Am. Inst. Chem. Eng. 39, 385-432 (1943)

Larcombe, H. L. M., "Centrifugal Dust Collectors" Min. Mag. 77, 137 (1947)

Lawrence, E. A., "Pressure Loss in Centrifugal Entrainment Separators under Vacuum" Chem. Eng. Prog. 48, 241-246 (1952)

Morgan, G. W., "Study of Motions in Rotating Liquid" Proc. Roy. Soc. 206, 108-130 (1951)

Plank, R., "The Centrifugal Jet" Refrig. Eng. 57, 448 (1949)

Reddick, H. W., Differential Equations, Second Edition, New York, John Wiley & Sons, 1949

Riegel, E. R., Chemical Machinery, New York, Reinhold, 1944, pp. 299-314

Roebuck, J. R., "A Novel Form of Refrigerator" J. App. Phy. 16, 285-295 (1945)

Scheper, G. W., "Vortex Tube. Internal Flow Data and Heat Transfer Theory" Refrig. Eng. 59, 985-989 (1951)

Smith, J. C., "Centrifuges" Chem. Ind. 65, 357-364 (1949)

Smith, J. C., "Selection of Centrifuges for Chemical Processing" Ind. Eng. Chem. 39, 474-479 (1947)

Stairmand, C. J., "Design and Performance of Cyclone Separators" Trans. Inst. Chem. Eng. 29, 356-372 (1951)

Stairmand, C. J., "Design and Performance of Cyclone Separators" Intern. Chem. Eng. and Process Inds. 33, 89-91 (1952)

Stairmand, C. J., "Sampling of Dust Laden Gases" Inst. Chem. Eng. (London) 29, 15-39 (1951)

Webster, D. S., "An Analysis of the Hilsch Vortex Tube" Refrig. Eng. 58, 163-171 (1950)

Weems, F. T., "Metallurgical Applications of the Dorr Clone" Min. Eng. TP3093B (1951)

Whiton, L. C., "Performance Characteristics of Cyclone Dust Collectors" Chem. & Met. Eng. 39, 150-151 (1932)

Yancey, H. F. and Greer, M. R., "The Cyclone as a Thickener of Coal Slurry" Trans. Am. Inst. Min. & Met. 177, 262 (1948); Coal Tech. TP2351 (1948)

APPENDIX

Determination of Orifice Coefficients

The flow of an incompressible fluid through an orifice has been found by experiment to be expressible by a mathematical equation of the form

$$y = a\ x^{1/2}$$

The method of least squares was used to treat the calibration data. The residual, R_n is given by

$$R_n = a\ x_n^{1/2} - y_n$$

The squared residuals of all points are summed up for a given orifice.

$$\sum R_n^2 = \sum a^2\ x_n - \sum 2\ a\ x_n^{1/2}\ y_n + \sum y_n^2$$

The minimum $\sum R_n^2$ is found,

$$\frac{\partial\left(\sum R_n^2\right)}{\partial a} = 2\ a \sum x_n - 2 \sum x_n^{1/2}\ y_n = 0$$

$$a \sum x_n - \sum x_n^{1/2}\ y_n = 0$$

$$a = \frac{\sum x_n^{1/2}\ y_n}{\sum x_n}$$

In the calculation of "a" for each orifice

y = flow, lb./sec.

x = manometer reading, in. Hg -in H_2O.

Orifice data are shown in Table X.

For the two oils that were metered, it was assumed that the orifice coefficients, C, in the following equations remained the same as for the water.

$$q = A\ C \sqrt{\frac{2g\ \Delta h}{1 - \bar{\beta}^4}}$$

where

q = flow rate, ft.^{3}/sec.

A = orifice area, ft.^{2}

C = coefficient

Δh = head across orifice, ft. fluid

$\bar{\beta} = \frac{D_2}{D_1}$

D_2 = orifice diameter

D_1 = pipe diameter, 2-inch std. pipe

From the calibration with water,

$$q = \frac{a}{\rho}\sqrt{\frac{12}{12.6}}\sqrt{\Delta h} = \frac{a}{\rho}\ x^{1/2}$$

$$q = \frac{a}{\rho}\sqrt{\frac{12}{12.6}}\sqrt{\Delta h} = A\ C\sqrt{\frac{2g}{1-\bar{\beta}^4}}\sqrt{\Delta h}$$

$$C = \frac{a}{\rho A}\sqrt{\frac{12\ (1-\bar{\beta}^4)}{25.2\ g}}$$

SAMPLE CALCULATIONS

1. Conversion of pressure drops from inches mercury minus inches water to pounds per square foot:

$$\Delta P = \frac{\Delta}{12} \left(\rho_1 - \rho_2\right) 62.4$$

where

Δ = manometer reading, inches

ρ_1 = specific gravity of mercury

ρ_2 = specific gravity of water

For the first point of Run X-1-A,

$\Delta = 0.20$ inches

$\rho_1 = 13.6$

$\rho_2 = 1.0$

$$\Delta P = \frac{\Delta}{12} (13.6 - 1)\ 62.4$$

$$= 65.5\ \Delta = 65.5 \times 0.20 = 13.1 \text{ lb./ft.}^2$$

2. Conversion of pressure drops from inches mercury minus inches oil to pounds per square foot:

$$\Delta P = \frac{\Delta}{12} \left(\rho_1 - \rho_{rt}\right) 62.4$$

where

ρ_{rt} = specific gravity of oil at room temperature

For the first point of run X-5,

$\Delta = 1.20$ inches

$\rho_{rt} = 0.92$

$$\Delta P = \frac{\Delta}{12} (13.6 - 0.92)\ 62.4$$

$$= 66.0\ \Delta = 66.0 \times 1.20 = 79.2 \text{ lb./ft.}^2$$

3. Flow rate calculation for water through N.E. inlet:

$$q = a\, v_f \sqrt{\Delta}$$

where

q = flow rate, ft.^{3}/sec.

a = calibration factor, lb./sec./in.$^{1/2}$

v_f = specific volume of water ft.^{3}/lb.

For run X-1-A,

$a = 4.89$ lb./sec./in.$^{1/2}$

$v_f = 0.0161$ ft.^{3}/lb.

$\Delta = 2.9$ inches

$$q = 4.89 \times 0.0161 \times \sqrt{2.9} = 0.134 \text{ ft.}^3\text{/sec.}$$

$$v_{iNE} = \frac{q}{\text{inlet area}} = \frac{0.134}{\frac{6 \times 0.317}{144}} = 10.1 \text{ ft./sec.}$$

4. Calculation of V_i:

$$V_i = \frac{v_{iNE} + v_{iSW}}{2}$$

For run X-1-A,

$$V_i = \frac{10.1 + 9.94}{2} = 10.02 \text{ ft./sec.}$$

5. Flow rate calculation for oil through N.E. Inlet:

$$q = A\, C \sqrt{\frac{2g\, \Delta h}{1-\bar{\beta}^4}}$$

For run X-5,

$A = 0.01211$ ft.^{2}

$C = 0.674$

$2g = 64.4$

$(1-\bar{\beta}^4) = 0.730$

$$\Delta h = \frac{\Delta}{12}\left[\frac{\rho_1 - \rho_{rt}}{\rho_o}\right]$$

ρ_o = specific gravity of flowing oil

Δ = 7.85 in.

ρ_o = 0.895

ρ_1 = 13.6

ρ_{rt} = 0.92

$$\Delta h = \frac{7.85}{12}\left[\frac{13.6 - 0.92}{0.895}\right] = 9.28 \text{ ft.}$$

$$q = 0.01211 \times 0.674\sqrt{\frac{64.4 \times 9.28}{0.730}}$$

q = 0.233 ft.^{3}/sec.

TABLE IX

ORIFICE CALIBRATION

Bottom Outlet Manometer Reading	Flow lb. per second	N.E. Inlet Manometer Reading	°F Water Temperature
5.15	11.0	4.65	81.5
4.00	9.81	4.10	83.3
6.70	13.00	--	82.4
8.45	14.3	8.65	80.6
9.50	15.4	10.05	78.8
5.70	11.6	5.85	77.0
4.30	9.53	3.60	75.2
1.60	6.33	1.45	75.2
2.65	7.72	2.55	90.5
4.00	9.30	3.95	84.2
6.75	13.0	7.20	80.6
8.80	14.9	9.40	77.0
10.40	15.9	10.30	75.2
Top Outlet		S.W. Inlet	
1.30	5.38	1.50	94.1
1.20	5.21	1.35	91.4
2.10	6.67	2.05	88.7
2.40	7.87	2.95	88.7
4.40	10.10	4.30	88.7
6.75	12.50	--	86.0
6.85	12.50	6.75	91.4
6.75	12.2	6.65	87.8
8.60	13.8	8.25	82.4
8.35	14.3	8.25	80.6
6.90	12.2	7.00	80.6
3.70	9.10	3.55	82.4
5.95	11.4	5.95	78.8
8.30	13.7	8.35	75.2
1.95	6.54	1.95	75.2
10.45	15.4	10.55	72.5

TABLE X

ORIFICE DATA AND PHYSICAL PROPERTIES
FOR OILS

ORIFICE DATA

Orifice	D_2 (in.)	a	C
N.E.	1.490	4.888	0.674
S.W.	1.490	4.751	0.655
Bottom	1.491	4.913	0.677
Top	1.490	4.763	0.657

PHYSICAL PROPERTIES

		SAE 10	SAE 60
Density g./c.c.	25°C.	0.9197	0.8947
	30		0.8918
	55	0.9001	
	60	0.8969	
	65	0.8948	
	70		0.8695
	80		0.8634
Viscosity cp	60°C.	14.2	
	70	9.94	53.6
	80		36.0

TABLE XI

PRESSURE DISTRIBUTION DATA FOR ALL RUNS

Temp. °C	Run No.	Manometer Readings In. Hg.-In. H_2O Top Outlet	Bottom Outlet	N.E. Inlet	S.W. Inlet	ΔP Manometer Reading In.Hg-In. H_2O	Tap No.	$\left(\frac{R}{r}\right)^2 - 1$
34.6	X-1-A	2.85	3.00	2.3	2.6	0.20	1	0.28
		2.78	3.00	2.9	2.6	1.60	2	1.04
		2.70	3.00	2.9	2.7	4.70	3	2.95
		2.65	2.98	2.9	2.6	9.40	4	6.02
		2.65	2.98	2.9	2.6	14.45	5	8.85
		2.65	2.98	2.9	2.6	14.80	6	8.62
		2.65	2.98	2.9	2.6	14.65	7	8.62
		2.65	2.98	2.9	2.6	14.25	8	8.62
		2,55	2.98	2.9	2.6	17.60	9	10.82
		2.55	2.98	2.9	2.6	21.30	10	12.97
34.6	X-1-B	4.20	4.25	4.5	4.35	0.75	1	0.28
		4.20	4.25	4.5	4.35	3.00	2	1.04
		4.20	4.25	4.5	4.35	8.25	3	2.95
		4.20	4.25	4.5	4.35	15.50	4	6.02
		4.60	4.25	4.5	4.35	23.65	5	8.85
		4.60	4.25	4.5	4.35	24.05	6	8.62
		4.60	4.25	4.5	4.35	23.60	7	8.62
		4.60	4.25	4.5	4.35	22.90	8	8.62
		4.30	4.15	4.5	4.35	28.85	9	10.82
		4.20	4.15	4.5	4.35	34.60	10	12.97
34.7	X-1-C	6.75	6.30	6.60	6.45	1.20	1	0.28
		6.15	6.30	6.60	6.45	4.30	2	1.04
		6.55	6.50	6.60	6.45	11.90	3	2.95
		6.55	6.40	6.50	6.45	22.35	4	6.02
		6.45	6.30	6.60	6.45	34.30	5	8.85
		6.45	6.30	6.60	6.45	35.40	6	8.62
		6.45	6.30	6.60	6.45	35.05	7	8.62
		6.45	6.30	6.60	6.45	34.20	8	8.62
		6.55	6.40	6.60	6.45	42.25	9	10.82
		6.45	6.35	6.60	6.45	51.40	10	12.97

TABLE XI

PRESSURE DISTRIBUTION DATA FOR ALL RUNS (continued)

Temp. °C	Run No.	Manometer Readings In.Hg. -In. H_2O Top Outlet	Bottom Outlet	N.E. Inlet	S.W. Inlet	ΔP Manometer Reading In.Hg- In. H_2O	Tap No.	$\left(\frac{R}{r}\right)^2 - 1$
35.7	X-1-D	8.0	8.30	8.65	8.55	1.50	1	0.28
		8.0	8.40	8.65	8.55	5.55	2	1.04
		8.35	8.50	8.65	8.55	15.30	3	2.95
		9.00	8.50	8.65	8.55	28.80	4	6.02
		8.65	8.50	8.65	8.55	44.30	5	8.85
		8.65	8.50	8.65	8.55	45.20	6	8.62
		8.65	8.50	8.65	8.55	44.95	7	8.62
		8.65	8.50	8.65	8.55	43.80	8	8.62
		9.90	8.50	8.65	8.55	54.50	9	10.82
		8.0	8.50	8.65	8.55	65.90	10	12.97
35.8	X-1-E	10.80	10.65	10.60	10.50	1.80	1	0.28
		11.30	10.65	10.60	10.50	6.70	2	1.04
		10.70	10.65	10.70	10.50	18.45	3	2.95
		10.90	10.65	10.60	10.50	34.75	4	6.02
		10.90	10.65	10.60	10.50	53.85	5	8.85
		10.90	10.65	10.60	10.50	54.75	6	8.62
		10.90	10.65	10.60	10.50	53.90	7	8.62
		10.90	10.65	10.60	10.50	52.45	8	8.62
		10.90	10.65	10.60	10.50	78.2	10	12.97
33.8	X-3-A	10.40	11.10	10.8	10.75	1.75	1	0.28
		10.35	11.30	10.8	10.85	6.60	2	1.04
		10.35	11.30	10.85	10.75	18.40	3	2.95
		10.35	11.30	10.85	10.75	36.30	4	6.02
		10.9	11.1	10.75	10.70	55.70	5	8.85
		10.60	11.1	10.95	10.75	68.70	9	10.82
		10.60	11.1	10.85	10.75	81.60	10	12.97
		10.60	11.1	10.85	10.75	56.00	6	8.62
		10.60	11.1	10.85	10.75	55.60	7	8.62
		10.60	11.1	10.85	10.75	54.40	8	8.62

TABLE XI

PRESSURE DISTRIBUTION DATA FOR ALL RUNS (continued)

Temp. °C	Run No.	Manometer Readings In. Hg. - In. H_2O Top Outlet	Bottom Outlet	N.E. Inlet	S.W. Inlet	ΔP Manometer Reading In.Hg- In. H_2O	Tap No.	$\left(\frac{R}{r}\right)^2 - 1$
37.0	X-4-A	2.55	2.70	2.50	2.50	0.45	1	0.28
		2.55	2.70	2.75	2.55	1.65	2	1.04
		2.55	2.70	2.65	2.55	4.50	3	2.95
		2.55	2.70	2.65	2.55	8.60	4	6.02
		2.55	2.70	2.75	2.55	12.95	5	8.85
		2.55	2.70	2.75	2.55	13.60	6	8.62
		2.55	2.70	2.75	2.55	13.80	7	8.62
		2.55	2.70	2.75	2.55	13.55	8	8.62
		2.55	2.70	2.65	2.55	20.00	10	12.97
		2.55	2.70	2.75	2.55	16.30	9	10.82
38.0	X-4-B	4.9	5.15	4.55	4.65	0.80	1	0.28
		4.9	5.15	4.55	4.65	3.10	2	1.04
		4.9	5.15	4.55	4.55	8.50	3	2.95
		5.00	5.15	4.55	4.55	16.35	4	6.02
		5.00	5.15	4.55	4.55	24.70	5	8.85
		5.00	5.15	4.55	4.55	25.80	6	8.62
		5.00	5.15	4.55	4.55	26.20	7	8.62
		5.00	5.15	4.55	4.55	25.95	8	8.62
		5.00	5.15	4.55	4.55	31.30	9	10.82
		5.00	5.15	4.55	4.55	38.45	10	12.97
38.0	X-4-C	6.7	6.65	6.20	6.25	1.15	1	0.28
		6.75	6.65	6.20	6.30	4.20	2	1.04
		6.7	6.65	6.20	6.25	11.30	3	2.95
		6.7	6.65	6.20	6.25	21.50	4	6.02
		6.7	6.65	6.20	6.25	32.55	5	8.85
		6.7	6.65	6.20	6.25	33.90	6	8.62
		6.7	6.65	6.20	6.25	34.40	7	8.62
		6.7	6.65	6.20	6.25	34.00	8	8.62
		6.7	6.65	6.20	6.25	41.10	9	10.82
		6.7	6.65	6.20	6.25	50.50	10	12.97

TABLE XI

PRESSURE DISTRIBUTION DATA FOR ALL RUNS (continued)

Temp. °C	Run No.	Manometer Readings In. Hg.-In. H_2O Top Outlet	Bottom Outlet	N.E. Inlet	S.W. Inlet	ΔP Manometer Reading In.Hg-In. H_2O	Tap No.	$\left(\frac{R}{r}\right)^2 - 1$
36.0	X-4-D	10.8	10.85	10.70	10.70	1.80	1	0.28
		11.0	10.85	10.60	10.70	6.70	2	1.04
		11.0	10.85	10.65	10.70	18.25	3	2.95
		11.0	10.85	10.65	10.70	34.70	4	6.02
		11.0	10.85	10.65	10.70	52.60	5	8.85
		11.0	10.85	10.65	10.70	54.40	6	8.62
		11.0	10.85	10.65	10.70	55.10	7	8.62
		11.0	10.85	10.65	10.70	54.40	8	8.62
		11.0	10.85	10.65	10.70	66.10	9	10.82
		11.0	10.85	10.65	10.70	81.20	10	12.97
38.5	X-4-E	11.6	11.70	11.40	11.45	1.95	1	0.28
		11.45	11.70	11.40	11.60	7.25	2	1.04
		11.6	11.70	11.40	11.60	19.70	3	2.95
		11.6	11.70	11.40	11.65	37.10	4	6.02
		11.6	11.70	11.40	11.65	57.00	5	8.85
		11.6	11.70	11.40	11.65	59.00	6	8.62
		11.6	11.70	11.40	11.65	59.80	7	8.62
		11.6	11.70	11.40	11.65	58.90	8	8.62
		11.6	11.6	11.25	11.60	70.10	9	10.82
		11.6	11.6	11.25	11.70	87.90	10	12.97

TABLE XI

PRESSURE DISTRIBUTION DATA FOR ALL RUNS (continued)

Temp. °C	Run No.	Manometer Readings In.Hg.- In. Oil: Top Outlet	Bottom Outlet	N.E. Inlet	S.W. Inlet	ΔP Manometer Reading In.Hg- In. Oil	Tap No.	$\left(\frac{R}{r}\right)^2 - 1$
60.8	X-5	7.6	8.0	7.85	7.85	1.20	1	0.28
		7.6	8.0	7.85	7.85	5.05	2	1.04
		7.6	8.0	7.85	7.85	14.07	3	2.95
		7.6	8.0	7.85	7.85	27.32	4	6.02
		7.6	8.0	7.85	7.85	41.30	5	8.85
		7.6	8.0	7.85	7.85	51.60	8	10.82
		7.6	8.0	7.85	7.85	61.92	9	12.97
		7.6	8.0	7.85	7.85	--	10	14.79
		7.6	8.0	7.85	7.85	45.7	6	8.62
		7.6	8.0	7.85	7.85	43.65	7	8.62
62.7	X-6	2.0	1.95	2.05	1.95	0.33	1	0.28
		2.0	1.95	2.05	1.95	1.35	2	1.04
		2.0	1.95	2.05	1.95	3.85	3	2.95
		2.0	1.95	2.05	1.95	7.56	4	6.02
		2.0	1.95	2.05	1.95	11.22	5	8.85
		2.0	1.95	2.05	1.95	14.31	8	10.82
		2.0	1.95	2.05	1.95	17.25	9	12.97
		2.0	1.95	2.05	1.95	29.67	10	14.79
		2.0	1.95	2.05	1.95	11.75	6	8.62
		2.0	1.95	2.05	1.95	11.93	7	8.62
61.5	X-7	4.7	4.6	4.7	4.7	65.20	10	14.79
		4.7	4.6	4.7	4.7	38.90	9	12.97
		4.7	4.6	4.7	4.7	32.15	8	10.82
		4.7	4.6	4.7	4.7	26.90	6	8.62
		4.7	4.6	4.7	4.7	25.60	5	8.85
		4.7	4.6	4.7	4.7	16.90	4	6.02
		4.7	4.6	4.7	4.7	8.65	3	2.95
		4.7	4.6	4.7	4.7	3.10	2	1.04

TABLE XI

PRESSURE DISTRIBUTION DATA FOR ALL RUNS (continued)

Temp. °C	Run No.	Manometer Readings In.Hg.- In. Oil: Top Outlet	Bottom Outlet	N.E. Inlet	S.W. Inlet	ΔP Manometer Reading In.Hg- In. Oil	Tap No.	$\left(\frac{R}{r}\right)^2 - 1$
60.2	X-8	4.5	4.15	4.35	4.35	61.65	5	8.85
		4.5	4.15	4.35	4.35	41.30	4	6.02
		4.5	4.15	4.35	4.35	21.50	3	2.95
		4.5	4.15	4.35	4.35	8.15	2	1.04
		4.5	4.15	4.35	4.35	2.20	1	0.28
		4.5	4.15	4.35	4.35	64.40	7	8.62
		4.5	4.15	4.35	4.35	76.35	8	10.82
		4.5	4.15	4.35	4.35	90.65	9	12.97
62.0	X-9	2.25	2.2	2.07	2.18	67.60	11	14.79
		2.25	2.2	2.07	2.18	68.50	10	14.79
		2.25	2.2	2.07	2.18	47.40	9	12.97
		2.25	2.2	2.07	2.18	40.70	8	10.82
		2.25	2.2	2.07	2.18	32.65	6	8.62
		2.25	2.2	2.07	2.18	32.20	5	8.85
		2.25	2.2	2.07	2.18	22.10	4	6.02
		2.25	2.2	2.07	2.18	11.45	3	2.95
		2.25	2.2	2.07	2.18	4.25	2	1.04
		2.25	2.2	2.07	2.18	1.15	1	0.28
63.0	X-10	1.55	1.25	1.13	1.17	35.80	11	14.79
		1.55	1.25	1.13	1.17	37.00	10	14.79
		1.55	1.25	1.13	1.17	25.40	9	12.97
		1.55	1.25	1.13	1.17	21.70	8	10.82
		1.55	1.25	1.13	1.17	17.75	6	8.62
		1.55	1.25	1.13	1.17	17.15	5	8.85
		1.55	1.25	1.13	1.17	11.90	4	6.02
		1.55	1.25	1.13	1.17	6.20	3	2.95
		1.55	1.25	1.13	1.17	2.30	2	1.04
		1.55	1.25	1.13	1.17	0.60	1	0.28

TABLE XI

PRESSURE DISTRIBUTION DATA FOR ALL RUNS (continued)

Temp. °C	Run No.	Manometer Readings In.Hg.- In. Oil: Top Outlet	Bottom Outlet	N.E. Inlet	S.W. Inlet	ΔP Manometer Reading In.Hg- In. Oil	Tap No.	$\left(\frac{R}{r}\right)^2 - 1$
73.2	X-11	3.65	4.15	4.15	3.80	75.7	9	12.97
		3.65	4.15	4.15	3.80	64.4	8	10.82
		3.65	4.15	4.15	3.80	52.5	7	8.62
		3.65	4.15	4.15	3.80	35.55	4	6.02
		3.65	4.15	4.15	3.80	18.1	3	2.95
		3.65	4.15	4.15	3.80	6.97	2	1.04
		3.65	4.15	4.15	3.80	2.05	1	0.28
		3.65	4.15	4.15	3.80	51.65	6	8.62
		3.65	4.15	4.15	3.80	50.9	5	8.85
		3.65	4.15	4.15	3.80	120.7	10	14.79
		3.65	4.15	4.15	3.80	112.6	11	14.79
		3.65	4.15	4.15	3.80	76.65	9	12.97
72.8	X-12	2.15	2.45	2.3	2.25	68.1	10	14.79
		2.15	2.45	2.3	2.25	62.6	11	14.79
		2.15	2.45	2.3	2.25	42.4	9	12.97
		2.15	2.45	2.3	2.25	35.4	8	10.82
		2.15	2.45	2.3	2.25	28.8	7	8.62
		2.15	2.45	2.3	2.25	28.3	6	8.62
		2.15	2.45	2.3	2.25	27.95	5	8.85
		2.15	2.45	2.3	2.25	19.2	4	6.02
		2.15	2.45	2.3	2.25	9.95	3	2.95
		2.15	2.45	2.3	2.25	3.8	2	1.04
		2.15	2.45	2.3	2.25	1.15	1	0.28
75.0	X-13	1.2	1.4	1.4	1.25	33.1	11	14.79
		1.2	1.4	1.4	1.25	35.55	10	14.79
		1.2	1.4	1.4	1.25	22.7	9	12.97
		1.2	1.4	1.4	1.25	15.1	6	8.62
		1.2	1.4	1.4	1.25	10.25	4	6.02
75.0	X-14	1.25	1.0	1.33	1.2	14.35	6	8.62
		1.25	1.0	1.33	1.2	9.7	4	6.02
		1.25	1.0	1.33	1.2	1.9	2	1.04
		1.25	1.0	1.33	1.2	21.7	9	12.97

TABLE XI

PRESSURE DISTRIBUTION DATA FOR ALL RUNS (continued)

Temp. °C	Run No.	Manometer Readings In.Hg.- In. H_2O Top Outlet	Bottom Outlet	N.E. Inlet	S.W. Inlet	ΔP Manometer Reading In.Hg- In. H_2O	Tap No.	$\left(\frac{R}{r}\right)^2 - 1$
27.3	X-15	1.60	1.65	2.00	1.90	75.9	10	14.8
		1.60	1.65	2.00	1.90	72.2	11	14.8
27.0		1.60	1.65	2.00	1.90	53.3	9	12.97
		1.60	1.65	2.00	1.90	45.2	8	10.82
		1.60	1.65	2.00	1.90	35.3	7	8.62
		1.60	1.65	2.00	1.90	34.4	6	8.62
		1.60	1.65	2.00	1.90	36.2	5	8.85
27.0		1.55	1.65	2.00	1.90	24.0	4	6.02
		1.55	1.65	2.00	1.90	12.5	3	2.95
		1.55	1.60	2.00	1.90	4.7	2	1.04
26.7		1.55	1.65	2.00	1.90	1.3	1	0.28
28.6	X-16-A	0.65	0.55	0.53	0.40	11.57	9	--
		0.65	0.50	0.53	0.40	10.02	8	10.82
		0.65	0.50	0.53	0.40	11.77	9	12.97
27.2		0.65	0.50	0.53	0.40	8.02	7	8.62
		0.65	0.50	0.53	0.40	7.81	6	8.62
		0.55	0.50	0.53	0.40	7.72	5	8.85
27.0		0.55	0.50	0.53	0.40	5.25	4	6.02
		0.55	0.50	0.50	0.40	2.72	3	2.95
27.0		0.55	0.50	0.50	0.40	1.03	2	1.04
		0.55	0.50	0.50	0.40	0.30	1	0.28
		0.55	0.50	0.50	0.40		10	
28.0		0.55	0.50	0.50	0.40		11	

TABLE XI

PRESSURE DISTRIBUTION DATA FOR ALL RUNS (continued)

Temp. °C	Run No.	Manometer Readings In. Hg.- In.H_2O Top Outlet	Bottom Outlet	N.E. Inlet	S.W. Inlet	ΔP Manometer Reading In.Hg- In. H_2O	Tap No.	$\left(\frac{R}{r}\right)^2 - 1$
26.0	X-16-B	3.35	3.30	3.85	3.75	136.75	11	14.79
		3.35	3.30	3.85	3.75	141.95	10	14.79
26.0		3.35	3.30	3.85	3.75	101.35	9	12.97
		3.35	3.30	3.85	3.75	86.30	8	10.82
26.0		3.35	3.30	3.85	3.75	67.20	7	8.62
		3.35	3.30	3.85	3.75	66.00	6	8.62
		3.35	3.30	3.85	3.75	69.10	5	8.85
26.0		3.30	3.30	3.85	3.75	45.60	4	6.02
		3.30	3.30	3.85	3.75	23.85	3	2.95
26.0		3.30	3.25	3.85	3.75	8.80	2	1.04
		3.30	3.25	3.85	3.75	2.40	1	0.28
	V-1	0.75	1.30	0.8	0.7	0.55	1	0.277
		0.75	1.30	0.8	0.7	1.85	2	1.039
		0.75	1.30	0.8	0.7	4.90	3	2.948
		0.75	1.30	0.8	0.7	9.35	4	6.017
		0.75	1.30	0.8	0.7	13.70	5	8.853
		0.75	1.30	0.8	0.7	13.60	6	8.622
		0.75	1.30	0.8	0.7	14.05	7	8.622
		0.75	1.30	0.8	0.7	17.60	8	10.820
		0.75	1.30	0.8	0.7	20.80	9	12.973
		0.75	1.30	0.8	0.7	30.30	10	14.793
		0.75	1.30	0.8	0.7	28.40	11	

TABLE XI

PRESSURE DISTRIBUTION DATA FOR ALL RUNS (continued)

Temp. °C	Run No.	Manometer Reading In.Hg.- In. H_2O Top Outlet	Bottom Outlet	N.E. Inlet	S.W. Inlet	ΔP Manometer Reading In.Hg- In. H_2O	Tap No.	$\left(\frac{R}{r}\right)^2 - 1$
	V-2	0.75	1.20	0.8	0.7	0.55	1	0.277
		0.75	1.20	0.8	0.7	1.80	2	1.039
		0.75	1.20	0.8	0.7	4.45	3	2.948
		0.75	1.20	0.8	0.7	8.25	4	6.017
		0.75	1.20	0.8	0.7	11.70	5	8.853
		0.75	1.20	0.8	0.7	11.50	6	8.622
		0.75	1.20	0.8	0.7	11.85	7	8.622
		0.75	1.20	0.8	0.7	15.0	8	10.820
		0.75	1.20	0.8	0.7	17.45	9	12.973
		0.75	1.20	0.8	0.7	25.45	10	
		0.75	1.20	0.8	0.7	24.10	11	
26.0	V-3	0.6	1.20	0.8	0.6	0.55	1	0.277
		0.6	1.20	0.8	0.6	1.80	2	1.039
		0.6	1.20	0.8	0.6	4.20	3	2.948
		0.6	1.20	0.8	0.6	7.60	4	6.017
		0.6	1.20	0.8	0.6	10.40	5	8.853
		0.6	1.20	0.8	0.6	10.25	6	8.622
		0.6	1.20	0.8	0.6	10.55	7	8.622
		0.6	1.20	0.8	0.6	13.55	8	10.820
		0.6	1.20	0.8	0.6	15.55	9	12.973
		0.6	1.20	0.8	0.6	22.15	10	14.793
		0.6	1.20	0.8	0.6	21.30	11	
27.0	V-1-A	0.2	0.25	0.60	0.40	0.28	1	0.277
		0.2	0.25	0.60	0.40	0.85	2	1.039
		0.2	0.25	0.60	0.40	1.90	3	2.948
		0.2	0.25	0.60	0.40	3.35	4	6.017
		0.2	0.25	0.60	0.40	4.40	5	8.853
		0.2	0.25	0.60	0.40	5.80	8	10.820
		0.2	0.25	0.60	0.40	6.60	9	12.973
		0.2	0.25	0.60	0.40	9.00	10	
		0.2	0.25	0.60	0.40	8.85	11	

TABLE XI

PRESSURE DISTRIBUTION DATA FOR ALL RUNS (continued)

Temp. °C	Run No.	Manometer Readings In.Hg.- In. H_2O Top Outlet	Bottom Outlet	N.E. Inlet	S.W. Inlet	ΔP Manometer Reading In.Hg- In. H_2O	Tap No.	$\left(\frac{R}{r}\right)^2 - 1$
27.0	V-2-A	0.15	0.35	0.55	0.30	0.30	1	0.277
		0.15	0.35	0.55	0.30	0.85	2	1.04
		0.15	0.35	0.55	0.30	1.95	3	2.95
		0.15	0.35	0.55	0.30	3.55	4	6.02
		0.15	0.35	0.55	0.30	4.80	5	8.85
		0.15	0.35	0.55	0.30	6.25	8	10.82
		0.15	0.35	0.55	0.30	7.15	9	12.97
		0.15	0.35	0.55	0.30	10.20	10	
		0.15	0.35	0.55	0.30	9.80	11	
27.5	V-3-A	0.09	0.35	0.52	0.30	0.30	1	0.277
		0.09	0.35	0.52	0.30	0.87	2	1.04
		0.09	0.35	0.52	0.30	2.10	3	2.95
		0.09	0.35	0.52	0.30	3.85	4	6.02
		0.09	0.35	0.52	0.30	5.35	5	8.85
		0.09	0.35	0.52	0.30	6.90	8	10.82
		0.09	0.35	0.52	0.30	8.05	9	12.97
		0.09	0.35	0.52	0.30	11.75	10	
		0.09	0.35	0.52	0.30	11.10	11	
27.5	V-4-A	0.11	0.33	0.49	0.30	0.30	1	0.277
		0.11	0.33	0.49	0.30	0.90	2	1.04
		0.11	0.33	0.49	0.30	2.30	3	2.95
		0.11	0.33	0.49	0.30	4.35	4	6.02
		0.11	0.33	0.49	0.30	6.25	5	8.85
		0.11	0.33	0.49	0.30	8.10	8	10.82
		0.11	0.33	0.49	0.30	9.50	9	12.97
		0.11	0.33	0.49	0.30	13.95	10	
		0.11	0.33	0.49	0.30	13.07	11	

TABLE XII

RESIDENCE TIMES FOR WATER IN THE CYLINDER

Run	Residence Time(s)	Flow lb. per Minute	Water Temp. °C
1	33.4	82.0	13.0
2	32.8	82.0	--
3	33.2	81.5	13.0
4a	4.0	476.0	12.4
4b	4.6	--	--
4c	4.0	--	--
5a	4.6	480.0	12.3
5b	4.5	--	--
5c	4.6	--	--
6a	4.6	483.0	12.2
6b	4.5	--	--
6c	4.3	--	--
7a	5.4	385.0	12.3
7b	6.0	--	--
7c	6.4	--	--
8a	6.0	388.0	12.2
8b	5.8	--	--
8c	6.0	--	--
9a	5.3	386.0	12.3
9b	6.4	--	--
9c	6.0	--	--
10	13.8	191.0	12.4
11	12.5	192.0	12.3
12a	13.2	191.0	12.3
12b	12.0	--	--
12c	12.7	--	--
13a	8.5	269.0	12.2
13b	9.0	--	--
13c	8.8	--	--
14a	9.0	269.0	--
14b	9.3	--	--
14c	9.7	--	--
15a	9.0	269.0	12.3
15b	9.0	--	--
15c	8.5	--	--

NOMENCLATURE

A = area, ft.^{2}

C = a constant

D_1 = inside diameter of pipe, 2.067 in.

D_2 = orifice diameter, in.

M = moment due to fluid friction, lb. force ft.

ΔP = pressure drop, P_R-p, lb. force/ft.^{2}

P_R = pressure at cylinder wall, lb. force/ft.^{2}

R = cylinder radius, ft.

R' = sphere radius, ft.

R_n = residual in method of least squares

V = resultant velocity, ft./sec.

V_i = average inlet velocity, ft./sec.

V_R = effective peripheral velocity, ft./sec.

V_o = total volumetric flow rate, ft.^{3}/sec.

a = a constant

g_c = conversion factor, lb. mass ft./sec.^{2}
lb. force

Δh = fluid head, ft.

h = cylinder depth, ft.

n = a constant

p = pressure at r, lb. force/ft.^{2}

q = orifice flow rate, ft.^{3}/sec.

r = position radius, ft.

r_2 = cylinder outlet radius, ft.

t = time, sec.

u = radial velocity, ft./sec.

v = tangential velocity, ft./sec.

v_f = specific volume, ft.^{3}/lb. mass

v_{iNE} = N.E. inlet velocity, ft./sec.

v_{iSW} = S.W. inlet velocity, ft./sec.

w = vertical velocity, ft./sec.

x = manometer reading, inches

y = flow rate, lb. mass/sec.

z = vertical distance, ft.

$\alpha = V_R/V_i$

$\beta = V_o \rho / 2\pi h \mu$

$\bar{\beta} = D_2/D_1$

Δ = manometer reading, inches

γ = specific shear, lb. force/ft.^{2}

μ = molecular viscosity, consistent units

ϵ = turbulent viscosity, consistent units

$\mathcal{E} = \mu + \epsilon$

$\nu = \mu / \rho$

ρ = fluid density, lb. mass/ft.^{3}

ρ_o = specific gravity of flowing oil

ρ_1 = specific gravity of mercury

ρ_2 = specific gravity of water

ρ_{rt} = specific gravity of oil at room temperature

ϕ = angular distance, radians